Development of a Portable Instrumentation System for *In Situ* Assessment of Soil Respiration

By
Florian Reumont

Department of Bioresource Engineering
Macdonald Campus of McGill University
Montreal, Quebec, Canada
September 2016

A thesis submitted to McGill University in partial fulfillment of the requirements of the degree of
Master of Science

ABSTRACT

Soil respiration measurement is an important tool in environmental studies and, less often, in agricultural applications. There exists various methods of measuring and quantifying this release of CO_2 from the soil surface. Currently, the three main working principles in point source measurement chamber designs are: closed dynamic chambers (or non-steady-state flow-through chambers); closed static chambers (or non-steady-state non-flow-through chambers); and open chambers (or steady-state flow-through chambers). These methods can be expensive and time consuming. The Rapid Soil CO_2 Analyzer (RSCA) developed in this project was built around a low-cost Non Dispersive Infrared (NDIR) sensor and aimed at providing a faster alternative to closed static chambers and a cheaper on to the closed dynamic and open chambers. The working principle shifted from passive air diffusion inside the chambers to forced extraction by the creation of negative pressure in the headspace. The RSCA reads and logs three-minute long, point-based sensor response measurements of CO_2 concentrations, temperature, humidity, and pressure in the headspace, as well as the location and time from the start of the trial.

The device was built and its main CO_2 sensor tested for this application. It was found to be accurate in stable conditions when compared to samples tested using a gas chromatograph equipped with a Flame Ionization Detector (FID) and an Electron Capture Detector (ECD). A dedicated software application in both MATLAB® and Python™ was developed to process the raw data from the device and extract the relevant defining parameters. The RSCA was tested in parallel to closed static

chambers at three different locations in southern Quebec. An attempt at modeling the RSCA data to relate it to the processed flux data of the static chambers was inconclusive as no strong correlation could be found. A controlled experiment was designed as a 2 by 4 factorial on homogenised soil, including two levels of compaction and four levels of moisture. Glucose was later added as a third factor in an attempt to push respiration levels to their potential maximums and magnify the differences. In result, the compaction x soil moisture interaction as well as the addition of glucose was found to have a significant effect on measured soil respiration at $p<0.05$.

RÉSUMÉ

La capacité à mesurer la respiration des sols est un outil important pour les études environnementales et, moins couramment, pour les applications agricoles. Diverses méthodes existent pour quantifier les émanations de CO_2 de la surface du sol. Il y a actuellement trois grands types de chambres, celles si sont : chambre dynamique fermé (ou chambre de circulation a état non-stable) ; chambre statique fermées (ou chambre de non-circulation a état non-stable) ; et chambre ouverte (ou chambre de circulation a état stable). Ces méthodes pouvant être coûteuses en argent et en temps, l'analyseur rapide de CO_2 du sol (ARCS) élaboré dans le cadre de ce projet visait à fournir une alternative plus rapide que les chambres statiques fermées et moins coûteuse que les chambres dynamiques fermées et ouvertes. Le principe de fonctionnement est passé de la diffusion passive de l'air à l'intérieur des chambres, à l'extraction forcée de l'air du sol par la création d'une pression négative dans l'espace libre de l'appareil. L'ARCS mesure et enregistre la concentration de CO_2, la température, l'humidité et la pression dans l'espace libre, ainsi que sa position et le temps depuis le début du test.

L'appareil a été construit et son principal capteur de CO_2 testé et jugé exact dans des conditions stables par rapport à des échantillons testés dans un chromatographe en phase gazeuse. Des logiciels MATLAB® et Python™ ont été mis au point pour traiter les données brutes provenant de l'appareil et pour créer des définitions de paramètres pertinents. L'ARCS a été testé en parallèle aux chambres statiques

fermées à trois endroits différents dans le sud du Québec. Une tentative de modélisation des données servant à relier le flux des chambres statique au résultat de l'ARCS ne donna pas de résultat concluant du fait de voir trop peu de paramètres inclus. Les résultats de l'expérience sur le terrain ne pouvaient être attribués avec certitude au prototype ou au système de chambre classique, une expérience contrôlée a été conçue en 2 par 4 factorielles avec deux niveaux de compaction et quatre niveaux d'humidité. Du glucose fut ajouté plus tard comme un troisième facteur dans une tentative de pousser les niveaux de respiration à leur potentiel maximum et agrandir les différences entre les traitements. L'expérience contrôlée a trouvé des résultats plus concluants, montrant que l'effet combiné de la compaction et l'humidité du sol ainsi que l'addition de glucose, a eu un effet significatif sur la respiration du sol à $p<0,05$.

ACKNOWLEDGMENTS

The author would like to acknowledge everyone who contributed at any level to the achievement of this dissertation. Funding for this research was provided in part through the Agricultural Greenhouse Gases Program of Agriculture and Agri-Food Canada. Many thanks are due to my colleagues of the Precision Agriculture and Sensor Systems (PASS) research team for their great help, support and source of inspiration in many parts of the project. Special thanks to Nandkishor Dhawale for drawing up the first concept of the RSCA; thank you to Ahmad Mat Su for his patient help in training me and for providing all the data processing software for the closed steady state chambers; thank you to Frédéric René-Laforest for his machining help and mechanical design insights; thank you to Hsin-Hui Huang for her general support in organisational and writing matters; thank you to Michael Saminsky, Bharath Sudarsan, Emeka Ngadi, and Francisco Ruiz de la Macorra for having, at one point or another, spent long hours with me sampling in the field; thank you to Kaitlin Lloyd and Cynthia Crézé for providing the raw closed steady state chamber data from St-Emmanuel and Sherrington research sites, respectively.

I am thankful to both Dr. Asim Biswas and my supervising committee member Dr. Joann Whalen for their advice and constructive criticism of my project as well as Dr. Chandra A. Madramootoo as the Project leader of the Agricultural Greenhouse Gases Program.

To my parents, brother and sister I would like to dedicate this thesis; without their support and encouragement, the first letter would never have been written.

Finally, I would like to express great gratitude and recognition to Dr. Viacheslav Adamchuk for his supervision and guidance which have always helped me advance, both in the project and personally. I am ever grateful for the opportunity he provided by offering me the chance to pursue this Master's Degree. I am glad I was able to learn from his knowledge, as well as experience his boundless enthusiasm for research. The atmosphere he created within his team was an open, jovial and hardworking one. I wish the best to all the people listed here, and all the others who at one point or another have helped me during the last few years, if only by lending an ear and nodding their head.

FORMAT OF THE THESIS

This dissertation, without being directly composed of past publications, is partially a reformatting of a published conference paper.

It is partially composed from papers written for courses during the completion of the Master's program requirements as well as a conference paper of the same title that was presented at the 2016 American Society of Agricultural and Biological Engineers (ASABE) Annual International Meeting in Orlando, Florida, USA. Parts of this dissertation will be used as a base for further journal publications.

CONTRIBUTION OF AUTHORS

The author of this thesis recognizes the many contributions of third parties to parts of the project. This thesis is due in no small part to the work of both Nandkishor Dhawale and Ahmad Mat Su who provided the original concept and much of the data processing, respectively. Dr. Viacheslav Adamchuk is the thesis supervisor and was actively involved in all stages of the project, providing advice and supervision. Dr. Adamchuk together with Dr. Joann Whalen also constituted the members of the supervising committee for this thesis. This study and its findings were presented at the annual Agricultural Greenhouse Gases Program (AGGP) meetings from 2014 to 2016, and at the 2016 Annual International ASABE Conference in Orlando, Florida, USA, both as an oral presentation and a conference paper.

TABLE OF CONTENTS

ABSTRACT ii
RÉSUMÉ iv
ACKNOWLEDGMENTS vi
FORMAT OF THE THESIS viii
CONTRIBUTION OF AUTHORS ix
TABLE OF CONTENTS x
LIST OF TABLES xiii
LIST OF FIGURES xiv
LIST OF ABREVIATION AND SYMBOLS xvii
Chapter 1: Introduction 1
1.1 General Introduction 1
1.2 Rational Statement 3
1.3 Research Objectives 4
Chapter 2: Literature Review 6
2.1 Science of Soil Respiration 6
2.2 Measurement Techniques 11
Chapter 3: Materials and Methods 17
3.1 The Rapid Soil CO_2 Analyser 17
3.1.1 System Development 17
3.1.2 Current Design 20
3.1.3 Data Collection Protocol 25
3.1.4 Data Processing 28
3.2 Sensor Testing 30
3.2.1 Introduction 30
3.2.2 Experimental Setup 30
3.2.3 Statistical Analysis 32
3.3 Field Testing 33
3.3.1 Agricultural Greenhouse Gases Program 33
3.3.2 Closed Steady State Chamber Design 34

3.3.3 Closed Steady State Chamber: Data Collection Protocol 36
3.3.4 Closed Steady State Chamber Data Analysis 37
3.3.6 Parallel Testing 39
3.3.7 Comparative Modeling 40
3.4 Controlled Experiment 41
3.4.1 Introduction 41
3.4.2 Experimental Setup 42
3.4.3 Data Collection 44
3.4.4 Data Processing 46
Chapter 4 Results and Discussion 48
4.1 RSCA Development 48
4.1.1 Results and Discussion 48
4.1.2 Design Improvements 50
4.2 Sensor Testing 51
4.2.1 Results 51
4.1.2 Discussion 55
4.2 Field Experiment 56
4.2.1 Results 56
4.2.2 Discussion 62
4.3 Controlled Experiment 65
4.3.1 Results 65
4.3.2 Discussion 67
Chapter 5 Conclusions 70
List of References 73
Appendices 80
Appendix A: Technical Drawings 80
A1- Drawing and important dimensions of main PVC cylinder for the RSCA 80
A2- Drawing and important dimensions of metal cutting disk for the RSCA 80
A3- Drawing and important dimensions of main delrin plate 81
A4- Drawing and important dimensions of delrin ECU slab 81
A5- Drawing and important dimensions of 3D printed relay protector (ABS) 82

A6- Drawing and important dimensions of 3D printed battery holder (ABS) ... 82
A7- Drawing and important dimensions of 3D printed battery holder (cover) (ABS) ... 83
A8- 3D render of first RSCA prototype ... 83
Appendix B: MATALB®, Python™, Arduino and SAS code ... 84
B1- RSCA Arduino code ... 84
B2- MATLAB® code for RSCA data processing ... 89
B3- Python™ code for modeling of first order response ... 93
B4- SAS code for section 3.1 Sensor Testing ... 94
B-5 SAS code for section 3.3 Field Experiment ... 95
B-6 SAS code for section 3.4 Controlled Experiment ... 96
Appendix C: Additional Data ... 98
C1- Drop in Pressure (hPa) results for the two factor factorial design with two levels of compaction and four levels of humidity. ... 98
C2- Change in CO_2 (ppm) results for the two factor factorial design with two levels of compaction and four levels of humidity ... 98
C-3 Change in CO_2 (ppm) results for the three factor factorial design with two levels of compaction, humidity and presence of glucose. ... 99
C-3 Drop in Pressure (hPa) results for the three factor factorial design with two levels of compaction, humidity and presence of glucose ... 99

LIST OF TABLES

Table 3.1: Selected model parameters 40

Table 3.2: Data table showing the wet and dry bulk densities (BD) as well as the gravimetric and volumetric water contents (WC) of the various treatments on each day of the experiment 44

Table 4.1: Price breakdown of the RSCA chamber by component 48

Table 4.2: Result of the unmodified linear regression modeling showing only included variables and their respective parameter estimate. The R^2, adjusted R^2 and RMSE of each model are also shown. 58

Table 4.3: Result of the linear regression modeling with ln(y) transformation, showing only included variables 61

LIST OF FIGURES

Figure 3.1: Original concept drawing of the RSCA..... 17

Figure 3.2: Picture of the first RSCA prototype using a built-in piston system..... 18

Figure 3.3: Picture of the second RSCA prototype using an external pump..... 20

Figure 3.4: Annotated latest RSCA design..... 21

Figure 3.5: Sensors and controller for the RSCA..... 22

Figure 3.6: Bottom view, position of sensors and sampling tube..... 23

Figure 3.7: Components of an NDIR CO_2 sensor..... 24

Figure 3.8: Flowchart of the Arduino Uno code for sampling process..... 27

Figure 3.9: Concentration curves from the all 24 trials of collected on Oct 12, 2015 at the Field 26 site. 29

Figure 3.10: Concentration curve from the 11^{th} trial of the data collected on Oct 12, 2015 at the Field 26 site shown as raw data (left) and as the concentration change with respect to the baseline (right). 29

Figure 3.11: Recorded sensor measurement (grey) and model fit (orange) for the 12^{th} trial of the data collected on Nov 12, 2015 at the Sherrington site..... 30

Figure 3.12: Side by side comparison of the working principles of the RSCA (left) and a classic, closed static chamber design (right). 35

Figure 3.13: Picture of non-steady state chamber and exetainers used for gas sampling, by Su (2016)..... 37

Figure 3.14: Proposed experimental setup where D is Dry, W is Wet, C is Compacted and NC is Non Compacted. G and NG represent respectively the presence of glucose and its absence..... 43

Figure 4.1: Box plot of the difference in CO_2 concentrations measurements of both measurement methods (GC and RSCA) at three time points (0, 45, and 150s) through sampling of 16 locations on a single day at the Field 26 location..... 51

Figure 4.2: Box plot of the difference in CO_2 concentrations measurements of both measurement methods (RSCA and gas chromatograph) at three time points (0, 45, and 150s) for the through sampling of 16 locations on a single day at the Field 26 location. 52

Figure 4.3: CO_2 concentrations of both measurement methods (RSCA and gas chromatograph) at three time points (0, 45, and 150s) through sampling of both the wet and dry treatments of the controlled experiment. 53

Figure 4.4: Time series of the CO_2 concentrations of both measurement methods (RSCA and gas chromatograph) at three time points (0, 45, and 150s) for 6 trials in lab conditions. 55

Figure 4.5: Correlation between humidity (top left), temperature (top right), pressure drop (bottom left), and CO_2 concentration change (bottom right) and the closed static chamber flux. 57

Figure 4.6: Scatter plot of the predicted vs the actual flux values, showing the trendline and R^2 for the unmodified model of all sites combined 58

Figure 4.7: Predicted VS Residual scatter plot before (top) and after (bellow) transformation from y to y' 59

Figure 4.8: Correlation between humidity (top left), temperature (top right), pressure drop (bottom left), and CO_2 concentration change (bottom right) and the transformed closed static chamber flux. 60

Figure 4.9: Scatter plot of the predicted vs the actual flux values, showing the trendline and R^2 for the model of all sites combined after natural log transformation of the response 61

Figure 4.10: Mean pressure drop for the four moisture levels for each of the two compaction levels. Bar height indicates the mean and error bars are +/- 1 standard error. Means sharing the same letter do not differ significantly at the 95% confidence level based on the Tukey mean comparison method 66

Figure 4.11: Mean CO_2 concentration increase for the four moisture levels for each of the two compaction levels. Bar height indicates the mean and error bars are +/- 1 standard error. Means sharing the same letter do not differ significantly at the 95% confidence level based on the Tukey mean comparison method 66

Figure 4.12: Mean CO_2 concentration increase for the wet and dry treatments at both compactions levels and with or without added glucose. Bar height indicates the mean and error bars are +/- 1 standard error. Means sharing the same letter do not differ significantly at the 95% confidence level based on the Tukey mean comparison method 67

LIST OF ABREVIATION AND SYMBOLS

AGGP	Agricultural Greenhouse Gases Program
ECD	Electron Capture Detector
C_m	Gravimetric concentration (mg m^{-3})
C_{ss}	Gas concentration at equilibrium (ppm)
C_t	Gas concentration at time t (ppm)
C_V	Volumetric gas concentration (ppm)
D/C	Dry compacted treatment
ECU	Electronic Control Unit
F26	Field 26 research site
FID	Flame Ionization Detector
f_t	Hourly flux in mg m^{-2} h^{-1}
G	Glucose treatment
GHG	Greenhouse gases
GPS	Global Positioning System
IR	Infrared
IRGA	Infrared Gas Analyser
M	Molecular weight
NDIR	Non-Dispersive Infrared
NG	No Glucose treatment
P	Maximum change in pressure (hPa)
ppm	Parts per million

RSCA	Rapid Soil CO_2 Analyser
SE	St-Emmanuel research site
SH	Sherrington research site
SOM	Soil Organic Matter
t	Time (s)
T	Temperature (°C)
W/NC	Wet Non-Compacted Treatment
WC	Water content (%)
α	Sensor time offset (s)
μ	Mean
τ	Time constant (s^{-1})

Chapter 1: Introduction

1.1 General Introduction

While soil respiration, namely the emission of carbon dioxide from the soil surface, is often measured with other greenhouse gases related to climate change, it is also a good indicator of many soil properties and as such, can also be of local interest to agricultural producers. Between 1990 and 2005, agriculture emissions increased by 17% globally and 32% in developing countries. This means that in 2005, the agricultural sector was responsible for 10-12% of the total anthropogenic emissions of greenhouse gases (Smith et al., 2007). These gases include methane (CH_4), nitrous oxide (N_2O) and carbon dioxide (CO_2). These are not equal in their quantities however as CH_4 and N_2O each respectively produced 3.3 and 2.8 $GtCO_2$-eq/yr (gigatonne carbon dioxide equivalent per year) out of the total 6.1 $GtCO_2$-eq/yr produced by the agricultural sector in 2005. CO_2 on the other hand only accounted for 0.04 $GtCO_2$-eq/yr showing that despite large gas exchanges between the soil and the atmosphere, the net flux of CO_2 can be considered roughly balanced. As such, the importance of soil respiration studies is approached here more with regards to field health and as a potential tool for studying the impact of various farming practices and field conditions on microbial activity in the soil. As soil respiration is affected by every possible soil property (organic matter content, temperature, humidity, etc.) any change in practices, irrigation or fertilizer use for example, will impact the soil's gas emissions (Luo & Zhou, 2006).

Equally as important as the greenhouse gases themselves are the techniques used to measure them. They can help to acquire a better understanding of the impact of different management practices across all range of soil types. However, soil respiration is extremely variable, both spatially and temporally, creating the need for long-term studies using accurate and rapid equipment. Such devices will usually sacrifice quality for price or vice-versa and are often quite cumbersome. This leaves an opening for a fast, inexpensive and reliable measurement technique, able to not only measure the respiration levels, but to also help understand their cause. The objective of this project was the creation of a portable system for soil respiration measurement that was both easy to use and fast while being as reliable as current high-tech systems. As such, the Rapid Soil CO_2 Analyser (RSCA) was developed. This device, using a combination of commercially available sensors and original design, was built and tested both in laboratory conditions as well as in various fields in the southern Quebec region throughout the summers of 2013 and 2015.

The RSCA was originally tested in parallel with a more classic method of soil respiration measurement. However, because of the double uncertainty inherent in performing field measurements while using another technique as method of comparison, the device was also tested within a controlled environment. This method of testing yielded clear differences in soil respiration magnitudes between applied soil treatments. Studies regarding soil respiration usually target specific sites and as such are meant to take into account the environmental factors of the location as well as the complexity of its soil horizons and temporal variations. The aim of this study is

not site specific but instead intends to validate a measurement technique. The amount of soil, granted that it can still provide ample amount of respiration, and the location from which it is taken therefore do not matter in the case of this controlled experiment where the soil is to mixed and homogenised. Testing for such a device will in fact be aided by repeatedly testing on the same soil, only varying one factor at a time.

The RSCA's working principle was aimed at shifting from the passive accumulation of air inside the chambers which proved to be time consuming, to an active method of air collection by the creation of a negative pressure in the headspace, effectively forcing the air out of the soil's pore spaces close to the surface. This was combined with a battery of sensors including: a volumetric Non Dispersive Infrared (NDIR) CO_2 sensor, a temperature and humidity sensor, a barometric pressure sensor, an ultrasonic sensor, a GPS unit and an SD card reader for data logging.

1.2 Rational Statement

This thesis proposes a new method and chamber design for *in situ* measurement of soil respiration. This new prototype is filling a niche in the currently existing chamber market by being both effective and low cost. Levels of carbon dioxide emissions from soil are a good indicator of microbial activity and overall health of the top soil. Such a portable chamber would find use in any agricultural and environmental research interested in the temporal and geospatial variability of soil respiration. The device could additionally be used in laboratory conditions as a multi-tool due to the variety

of included on-board sensors. The addition of a GPS unit to the device also allows for the creation of georeferenced soil respiration maps potentially helping in data analysis or in the creation of more traditional prescription soil treatment maps.

1.3 Research Objectives

The main goal of this thesis was the development and testing of the Rapid Soil CO_2 Analyser (RSCA). This progression can be broken down into four experiments: (1) The prototyping and development of the RSCA itself, (2) the validation of the main NDIR CO_2 sensor against gas sampled and analysed via a gas chromatograph, (3) the parallel testing of the RSCA against the closed static chambers used during the AGGP project and (4) the testing of the RSCA in a controlled laboratory environment to induce extreme differences in obtained data.

The objective of the first section was the prototyping of the device itself. The aim in this case was the development of a portable chamber including a CO_2 sensor with the aim to vacuum soil air out and directly measure CO_2 concentration dynamics *in situ*. The main design constrains of the project were the portability of the chamber, its ease of use, its reliability and its accuracy, all while maintaining a low construction cost.

The second section's objective, namely, the validation of the chosen CO_2 sensor was to be performed alongside the other tests. The aim of this section was to sample the headspace of the RSCA at regular intervals of its sampling cycle and compare the data

obtained from the prototype with the air samples analysed in a gas chromatograph. This would be a crucial step in validating any further data obtained from the device.

The objective of the third section was aimed at relating the data obtained from the RSCA device with the ones gathered through a more classical method of soil respiration measurement. This was to be done by collecting data at three fields in southern Quebec alongside the classic, closed static chambers that were used for sampling during the course of the Agricultural Greenhouse Gas Program, funded by Agriculture and Agri-Food Canada. While the working principle of the RSCA made it impossible to directly obtain flux readings, the aim of this experiment was the creation of a model to relate the RSCA data to the flux values obtained from the classic chambers.

The fourth and final section of this thesis was undertaken due to difficulties with data fluctuations hampering the creation of the aforementioned model. To remedy this, a controlled experiment created, using homogenous soil and controlling the exact levels of compaction and volumetric water content. The objective of the experiment was to induce a drastic change in soil respiration levels from a soil sample so as to obtain clear responses in sensor readings. This identification work then permitted the means of working backward and understanding the more complex effects of a real field through the patterns of the collected data.

Chapter 2: Literature Review

2.1 Science of Soil Respiration

Soil respiration, often erroneously simplified as the CO_2 exchange through the soil surface, is a term encompassing both the production of CO_2 and its transport from the soil to the atmospheres. The production of CO_2 is a biochemical process originating from the root of plants along with the microorganisms and heteroclite fauna living in the soil and litter layers. This production can originate from both aerobic environments, by way of the Tricarboxylic (TCA or Krebs) cycle, or from anaerobic ones such as wetlands and waterlogged soils, where glucose is fermented to organic acids, and methanotroph oxidize methane (creating carbon dioxide). In standard agricultural conditions, while both conditions will often occur at different points in time, aerobic environments are usually more common. In these, glucose is oxidized by living organisms to create energy, carbon dioxide being a by-product of this chemical reaction. The rate of this process is regulated by a combination of energy demand, substrate availability, oxygen supply and temperature. While strongly impacted in the short run, an organism's respiratory capacity will often adjust in the long run, especially with regards to temperature (Atkin Owen & Tjoelker, 2003). Attempting to balance its growth, and hence, its need for energy, with the available resources.

As for the sources, plant roots are considered to account for approximately half of the total soil respiration; of course, this is heavily dependent on the properties of the

study field. This means that there exists a significant correlation between overall soil respiration and root density along a soil gradient (Hanson et al., 2000). Around the roots of a plant lay the rhizosphere, as introduced by Richards (1987). In this 10 to 20 μm thick layer, soil organisms thrive and it is where much of the microbial activity and as such, heterotrophic, or soil organic matter (SOM) decomposition happens. This bacteria is heavily reliant on the substrates exuded by the roots which act as their main growth limiter (Vance & Chapin, 2001). This microfauna can also be found decomposing SOM in the litter of a field, which, while often disregarded during soil respiration studies for environmental purposes, has been found to increase the total soil respiration by up to 30% in some studies (Wang et al., 1999) . Additionally, litter can be considered the respiration layer which is most affected by climatic factors. Annual mean temperature, mean precipitation and annual actual evapotranspiration have all been found to affect the SOM decomposition rates inside a field (Fogel & Cromack, 1977). These factors often are considered interdependent and compounding, especially between temperature and moisture (Wildung et al., 1975; Witkamp, 1966).

While the production aspect of soil respiration lays in the biochemical sector, its transport to the surface layer and the gas exchange with the atmosphere is mostly dictated by field conditions and the physical factors of the soil (texture, water content, bulk density, etc.). While CO_2 is produced mostly in the top soil, its concentration is often higher deeper within a soil profile, as found by Lewicki et al. (2003). In two California sites, the concentrations were between 320 and 1000 μmol^{-1} in the surface

layers (~10cm) and 17,500 to 32,000 μmol^{-1} in the deep soil (up to 80cm). This is partially due to CO_2 leaching into the groundwater and percolating down with it, storing itself deeper into the soil. Additionally, the movement of CO_2 in the soil via diffusion is a slow process, creating a buildup in the deeper layers. This ultimately creates a strong concentration gradient within the soil, allowing the CO_2 to move up through, and out of, the soil by mass flow or diffusion. This gradient is affected by soil texture, precipitation/water infiltration and the ratio of CO_2 production versus movement rate. The movement itself has been found to occur through a continuous network of air filled pores connecting the deeper layers of the soil to its surface (Hillel, 1998). The mass flow itself can occur through various mechanisms ranging from changes in atmospheric pressure and temperature, causing the air to expand and contract, to rainwater infiltrating the soil and replacing the air within, expelling it through the surface. Other processes including surface wind gusts, fluctuating water tables (pushing or pulling air with their rise and fall) or tillage and compaction done by agricultural machinery (Rolston, 1986).

Understanding the creation and transportation process allows us to identify the main factors controlling soil respiration. The first and foremost being substrate availability, as without it, plants and microbes could not thrive in the soil. While the rate of soil respiration can be linearly correlated with substrate availability, the exact rate of this conversion varies with substrate types (Berg et al., 1987). Simple sugars may be converted quickly and easily while more complex humic acids can have residence times of hundreds or thousands of years. While the large variety of substrate makes

it difficult to derive relationships between their supply and respiratory CO_2, experiments have shown this effect by limiting the substrates from canopy photosynthesis and measuring drastic drops in soil respiration of between 50 and 70% (Craine et al., 1999; Hogberg et al., 2001). Related to this is the second and usually most relied upon factor for estimating the magnitude of soil respiration - temperature. As shown by Burton et al. (1996), autotrophic respiration (roots and rhizosphere), which makes up for half of the total respiration, increases exponentially with temperature. At low temperatures, enzyme activity is a major limiting factor while at high levels, enzymes become denatured and the respiration depressed. In the mid-ranges, however, temperature is often considered to have an exponential relationship with biochemical processes in the soil (Hoff, 1884). As such, the temperature effect can be summarised by an exponentially increasing slope, from its low limiting values of the biological zero of 5°C, to its non-limiting state where substrate availability becomes more important, to finally reaching its denaturation point where enzymes get irreversibly damaged and soil respiration decreases once again.

Influencing soil respiration in a different manner, soil moisture increase and decrease in a field has been debatably correlated with soil respiration levels. While Martin and Bolstad (2005) show that even 9% difference in mean soil moisture during a drought year can have a negative effect of up to 15 % of the CO_2 emissions. Other studies such as Ruser et al. (2006) proclaim they saw no effect of various moisture levels on CO_2 emissions throughout differently compacted soils. Dörr and Münnich (2011)

advanced a reasonable explanation that soil moisture in fact changes the temperature sensitivity of soil respiration. While their study shows lower emissions during the wet years, this is contradicted by various other studies showing lower emissions in well drained sites (Davidson et al., 2000; Xu & Qi, 2001). At the extremes, both are considered to be true, as dry soil will create a water limiting environment for microbes while a high percentage of water filled pore space will drastically decrease the aeration of the soil, creating anaerobic conditions. The shape of the optimum point is a debatable issue with authors such as Papendick and Camprell (1981) proposing a singular point preceded and followed by a quick decrease in soil respiration. While others, such as Liu et al. (2002), describe an optimum plateau, allowing for a wider range of water content levels before seeing a drop-off in soil respiration.

Other related factors affecting soil respiration include the already mentioned oxygen level of the soil, which can become a main limiting factor in wetlands and flooding areas (Crawford, 1992). When this happens, root respiration of plants such as the *Senecio aquaticus* growing in anoxic conditions will be one third of that of the aerated culture (Lambers & Steingrover, 1978). Another factor is the nitrogen concentration in the soil. High levels of nitrogen have been linked to high protein contents (~90%) leading to high maintenance respiration for protein repair and replacement (De Vries, 1975). As such, a high nitrogen content is commonly associated with higher growth rates, and hence, respiration. Soil texture is also considered important in the transport phase of the soil respiration process. This is mainly due to its relation with soil porosity which in turn impacts soil moisture, aeration and overall fertility.

Microbial growth and hence, respiration is also affected by soil texture as was shown in laboratory tests by McInerney and Bolger (2000), where clayish soils produced 20-40% less CO_2 than silty loam soils at room temperature. Kowalenko et al. (1978) also observed a 50% greater CO_2 production from clay loam soils than from sandy soils.

Soil temperature, moisture and aeration can all be affected by the type of management practices used in the field. As attested by many studies, compaction, or short-term no-till, can result in poor aeration, waterlogging and hence, anaerobic conditions, reducing both microbial and root respiration (Linn & Doran, 1984; Rice & Smith, 1982). Over the long term, however, less intensive tillage operations such as no-till or strip tillage with careful irrigation management would reduce CO_2 emissions overall (Eshel et al., 2014; Jabro et al., 2008) . Other studies showed the tillage impact on the topsoil temperature, with Han et al. (2014) showing that minimal tillage and no-till applications reduced the thermal amplitude in the top 15 cm and increased its temperature by 0.5-2.2°C. While understanding how CO_2 is created and transported in the soil is a crucial step, measuring the output of a soil can be equally as important for environmental and agricultural studies.

2.2 Measurement Techniques

Methods of soil GHG measurements are important in acquiring a better understanding of the impacts of different management practices across all range of soil types. *In situ* soil respiration is extremely variable, both spatially and temporally (Currie, 1974), creating the need for long-term studies using accurate and rapid

equipment. The way to perform these studies often depends on the type of measurement methods (and hence measurement devices) available to the researcher. Some are more suited to certain situations than others. As a gas is being measured in all cases, all working principles involve an enclosed space, hence, the nomenclature of "chambers" is often used to describe the various contraptions.

Measurement methods can be classified according to the chamber's working principle. Each different measurement technique has varying benefits and drawbacks. The three main working principles in chamber design are: closed dynamic chambers (or non-steady-state flow-through chambers); closed static chambers (or non-steady-state non-flow-through chambers); and open chambers (or steady-state flow-through chambers) (Pumpanen et al., 2009). The original design for soil CO_2 measurement by Henrik Lundergardh (Lundergardh, 1922), a simple collard glass bell sampled for air at regular time intervals, was later coined to be of the closed static method as it had no exchange with the air outside the device. Variations of this method are still commonly used as they are inexpensive and the chambers simple to construct. The gas thus sampled is then analyzed in a laboratory, usually using gas chromatography (GC) along with the appropriate detector (Pavia et al., 1988).

This original method was found to be flawed in that an increased concentration of CO_2 inside the chamber would slow down the diffusivity from the soil to the chamber. The first open dynamic chambers by Porkka (Porkka, 1931) were meant to resolve this issue by continuously pumping air through the chamber until the CO_2 concentration

at the outlet reached a steady state and the flux could be determined by knowing the initial-exterior air concentration, the area of the chamber, and the flow through rate. This created the first open system. While not very common after their debut because of the difficulty in creating mobile facilities to pump and analyze the air, these have more recently become available due to the miniaturization of both electronics and power source components, lowering their price and size.

Along with these improvements came the second generation of closed chambers, where, as opposed to trapping the target gas in $Ba(OH)_2$ or absorbing it in NaOH or soda lime and titrating them thereafter, the gas was to be constantly cycled through an on-site analyzer to obtain quicker results. These are nowadays often infrared gas analysers (IRGA) and work using the non-dispersive infrared (NDIR) principle explained in Section 3.1.2. Gas chromatograph with the adequate detectors also exist in portable formats capable of in-situ measurements (Rochette & Hutchinson, 2005). The difference between closed and dynamic systems is at present, more a matter of price and portability as GC machines and IRGAs can be used in both systems with the only difference one is in the lab as opposed to in the field; the working principle and the chamber design is in essence the same.

Currently available commercial products span the whole range of working principles for gas chambers. The LI-8100A chamber system from LI-COR (LI-COR Inc., Lincoln, NE, USA) and SRC-1 from PP Systems (PP Systems International Inc., Amsbury, MA, USA) are examples of closed dynamic chambers, calculating the rate of increase of CO_2

inside the chamber by re-circulating the air through an IRGA. These commercial chambers are usually quite advanced but can fetch a high price. On the opposite side are closed static chambers which are used in many studies; these are more often self-built due to their simplicity and relative low material cost. Open chambers are rarer to find commercially due to their higher complexity and many are associated with potential issues. The Rapid Soil CO_2 Analyzer (RSCA) chamber discussed in this thesis was developed to fill the niche of a low cost rapid system that would be both portable, accurate and fast.

With regards to measuring soil respiration, chamber reliability and accuracy is, along with model discussions, where most scientific interest is to be found. While many methods and products flaunt their ability to precisely detect absolute levels of concentration, most are often considered to be underestimating the actual values (Davidson et al., 2002) even up to around 35% (Healy et al., 1995; Pumpanen et al., 2004; Smith et al., 2003). Additionally, Davidson et al. (2002) warns of the large errors which can occur from over or under-pressurization of the classic chambers as the former will impede the flow from the soil to the chamber while the later will artificially enlarge the measurement. The comparison between chamber methods will often simply state whether they generally over or underestimate measurements relative to one another (Nay et al., 1994). These errors in estimation can come from many sources such as ignoring or wrongly modeling diffusion of the gas in the chamber (Livingston et al., 2005). Even underestimating the impact of a bad air seal such as explained by Hutchinson and Livingston (2001) who not only point out the

importance of a properly sized air vent for the chamber being used, but look further into chamber building by showing numerically why, for example, the depth of insertion minimizing gas loss by lateral diffusion is smaller than ordinary in compacted, wet or finely textured soils, but much larger in highly porous soils. They also state that "repetitive sampling at the same location is not a major source of error when using non-steady-state chambers", this being an important consideration when attempting to do repeatability tests for instrument validation. Allowing for repeated field measurements without the need to displace the equipment, as, moving to another location, even adjacent, may induce changes in soil properties and hence, respiration. An additional consideration in creating experimental designs with spatial replicates of chambers comes from Rochette et al. (1991) who, studying two agricultural fields under different crops, found that the spatial variability of soil respiration occurred at a scaler smaller than 15 cm. Also finding that the soil released significantly more CO_2 form its surface in the row than in the interrow. Hence replicates for a point should be performed no further than in a 15 cm radius around each other, lest they show some significant variability.

No matter the sampling mechanism, the CO_2 emissions still respond to the same factors as they do naturally. Historically, having been only correlated with soil temperature, especially in biogeochemical models (Davidson et al., 2006), CO_2 emissions are understood as the result of multiple sources and complex interactions between internal and external soil factors such as: humidity (Schlentner & Cleve, 1985; Singh & Gupta, 1977); soil porosity (linked to compaction levels); organic

matter; and vegetation cover (Raich & Tufekcioglu, 2000). The need to include such factors in the most recent formulas came from the unexplainable variations obtained when using the classic temperature models. Properly factoring in these additional variables is still difficult and as such, carbon emissions from the soil are still one of the least understood natural factors with predictions from the various measurement instruments obtaining different absolute values. However, soil temperature remains the most easily explained factor, correlating with an exponential increase in soil respiration with most error happening at the lower temperature ranges (Fang & Moncrieff, 2000). Models based solely on temperature are only suited however to understanding the relative difference in respiration as temperature changes. The absolute value of respiration can only theoretically be found or approximated by knowing all other affecting factors.

Chapter 3: Materials and Methods

3.1 The Rapid Soil CO_2 Analyser

3.1.1 System Development

The RSCA development began in the summer of 2013 and saw continuous changes and improvements up to the end of the project. Of these, three main versions can be identified. The original concept of the RSCA can be seen in Figure 3.1. At this stage the chamber was designed to press into the soil and measure the CO_2 concentration at the soil surface. The chamber would ideally come equipped with both a temperature and humidity sensor as well as a fan for air mixing. The CO_2 sensor would then be rinsed with clean air after use. A pressure equalizing opening would keep the air inside the chamber at the 1 atm pressure, ideal for gas sensing. This version of the design was quickly abandoned due to flaws in the soil compression concept as well as an unnecessary complexity in the spring and top plate design.

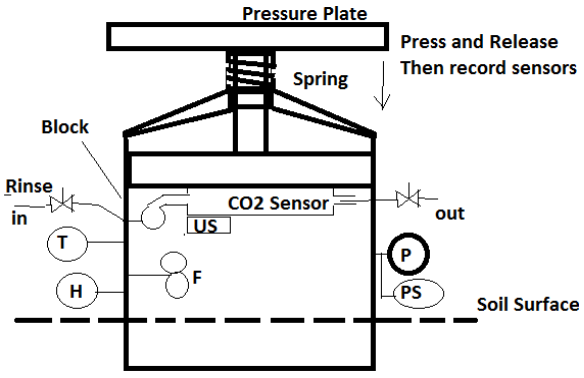

Figure 3.1: Original concept drawing of the RSCA

The first built prototype of the RSCA used a different working principle than the original concept. Instead of pressing into the soil, the chamber was devised to vacuum

the air from the soil and into the headspace of the chamber. This version can be seen in Figure 3.2. The main physical difference which can be noticed when compared with the concept drawing are the simplified piston as well as the addition of an electronic control unit (ECU) to manage the various sensors and give control to the user over the start and end of sampling.

Figure 3.2: Picture of the first RSCA prototype using a built-in piston system

The main delrin plate, then a piston, was made airtight by inserting two large plastic O-rings in grooves on its perimeter. The handle was screwed directly into the plate without going through it and held in place by a nut to prevent movement from damaging the grooves in the plate. During sampling, the handle and plate would be pulled up, creating suction directly inside the chamber. This idea was later abandoned as such a large piston was difficult to uniformly pull as well as being difficult to be made fully airtight due to the size of the O-rings. This method was considered too temperature dependent as the O-rings would shrink in cold weather, leaving gaps for

air to pass, and expend if warm, making the manual pull difficult, causing inconsistencies in the vacuuming process, and hence, random errors in the data.

The second prototype of the RSCA was the result of the need to fix numerous issues found in the testing of the first version. The original prototype lacked the inclusion of a digital pressure sensor, hence, it did not take into account the pressure dependency of the CO_2 sensor. The design also did not include an on-board GPS unit. This omission created a situation where mistakes in data gathering were additionally punishing. As, bar the use of an external handheld GPS unit, taking too many or too few measurements than intended could cause serious complication during data analysis phase. Hence, the sampling had to be done in a separately recorded sequence with a known number of replicates per site. This allowed for no mistakes from the user or random faults in the chamber. Another significant difference was the switch between a single 9-V alkaline PP3 battery and 6 1.5-V AA batteries in series. This lead to an output of similar voltage but at a more constant amperage so as to last longer in the field and cause fewer faults in the sensors.

The most noticeable difference, however, was the switch from the original piston system to an external, commercial, double-action hand pump. This change came about because of the difficulty in creating a sealed headspace in the first prototype. Instead, the piston was fixed in place and made airtight. Additional minor changes were made to the design, such as a 3D printed holder for the power source and a change in the Electronic Control Unit (ECU) housing to accommodate for the GPS unit.

While an upgrade from the previous version, the external pump was later abandoned due to variability in the negative pressure created in the headspace caused by even slightly different pumping speeds. This second version of the RSCA can be seen in Figure 3.3.

Figure 3.3: Picture of the second RSCA prototype using an external pump

3.1.2 Current Design

The current version of the RSCA is built upon a 20.32 cm (8 in.) diameter PVC cylinder, 15.6 cm (6.14 in.) high. The exterior of the cylinder is fitted at the bottom with a 2.5cm (~1 in.) metal cutting blade for soil penetration and seal. A delrin plastic wheel was installed and sealed 7.5 cm (~3 in.) from the bottom of the PVC cylinder to create an enclosed headspace inside the chamber. The delrin plate was drilled to allow for the wiring of the various sensors fitted to the underside of the plate as well as a 1 cm (0.4 in.) diameter hole fitted with an ID 0.8-cm tube linked directly to the pump's air intake. This allowed for the creation of negative pressure inside the headspace. The ECU along with an electrical, battery driven, commercial air pump (Intexcorp, Long

Beach, CA, USA), are both located on a delrin slap mounted across the PVC cylinder to provide space for cables and pipes. An annotated cross section rendering and picture of the chamber are shown in Figure 3.4. The chamber holds a headspace of 5.4 L, all of which are replaced by the pump flow during the time it is on. The volumetric air replacement of the pump in field conditions will also heavily depend on soil porosity as it dictates the intensity of the created drop in pressure. As an added note, the chamber was built using chest locks, bayonet connectors and easily removable screws to enable upgrades and modifications to be implemented gradually and modularly. This has helped in creating the current chamber, a third version prototype using the same core of materials as its predecessors but improving its ease of use and automation.

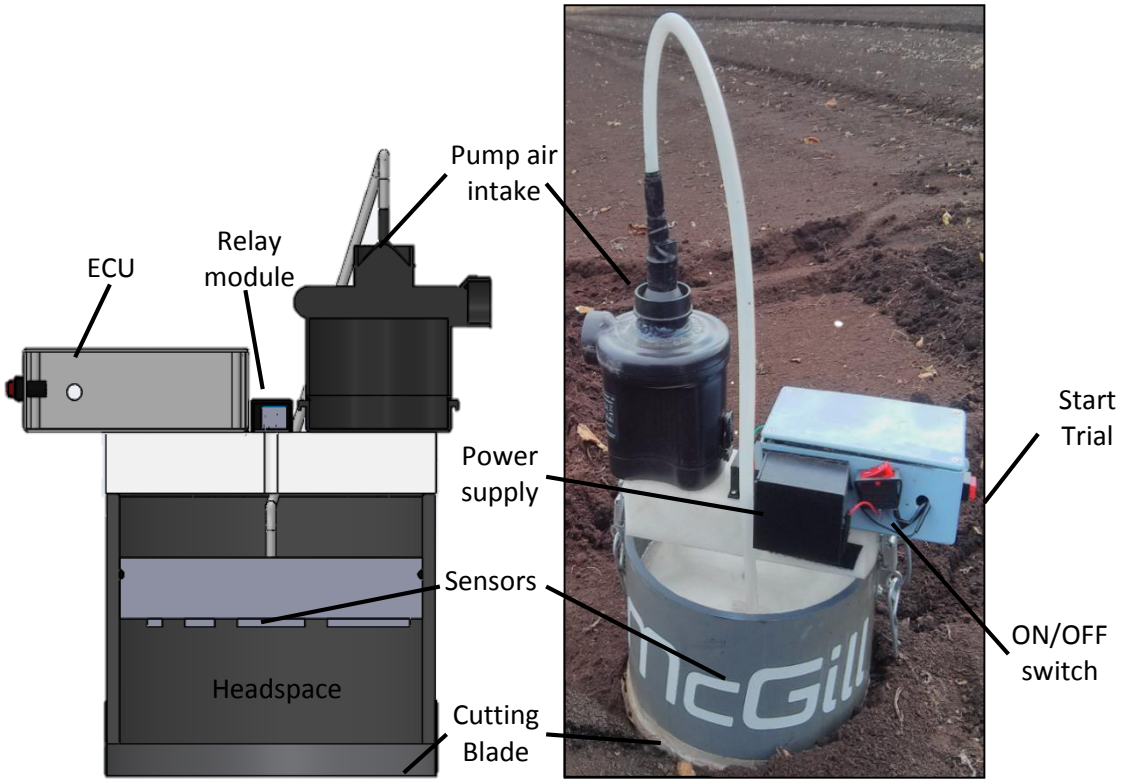

Figure 3.4: Current RSCA design

The data acquisition system of the RSCA is composed of a battery of sensors controlled through the ECU. The ECU primarily consists of an Arduino Uno microcontroller (Revision 3) mounted with an Adafruit Ultimate GPS shield (Adafruit Industries, New York City, NY, USA), sporting an FGPMMOPA6H GPS chip (GlobalTop Technology, Tainan City, Taiwan) and a micro SD card (Kingston Technology, Fountain Valley, CA, USA) slot for data logging. A sensor shield is also fitted on the microcontroller for ease of connection with the various sensors. A button is mounted on the ECU's box for the user to start the trial. The length of the trial is then indicated by an LED for feedback on the current state of the device. This control setup can be seen in Figure 3.5.

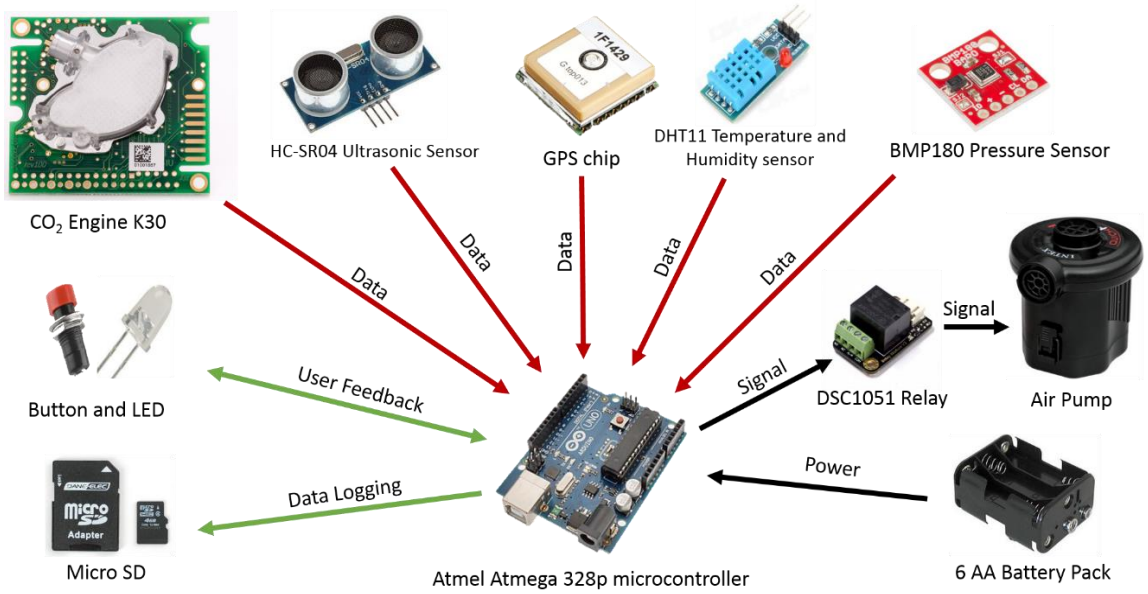

Figure 3.5: Sensors and controller for the RSCA

The headspace of the RSCA houses a CO_2 Engine K30 sensor (SensAir AB, Delsbo, Sweden) for measuring CO_2 concentration in the air (ppm); a DHT11 (Aosong Electronics Co., Ltd, Tenhe Town, Guangzhou, China) for measuring air temperature

(°C) and relative humidity (%); a Paralax ping Ultrasonic sensor (Parallax, Inc., Rocklin, CA, USA) and a BMP180 (Robert Bosch GmbH, Gerlingen, Germany) barometric pressure sensor (hPa). The headspace of the chamber also houses a fan for air mixing as well as a sampling tube for air sampling. The ECU is powered through 6 AA batteries connected in series creating a 9V supply. The sensors are powered at 5V via the ECU (the Arduino microcontroller having a built-in linear regulator to step down the voltage). The electrical pump is controlled via a relay module, turning it on and off automatically. The pump, the relay and the ECU are mounted on the delrin plate above the PVC cylinder. The whole setup is turned on and off manually trough a switch on the side of the ECU. The sensors' positions on the delrin plate can be seen in Figure 3.6.

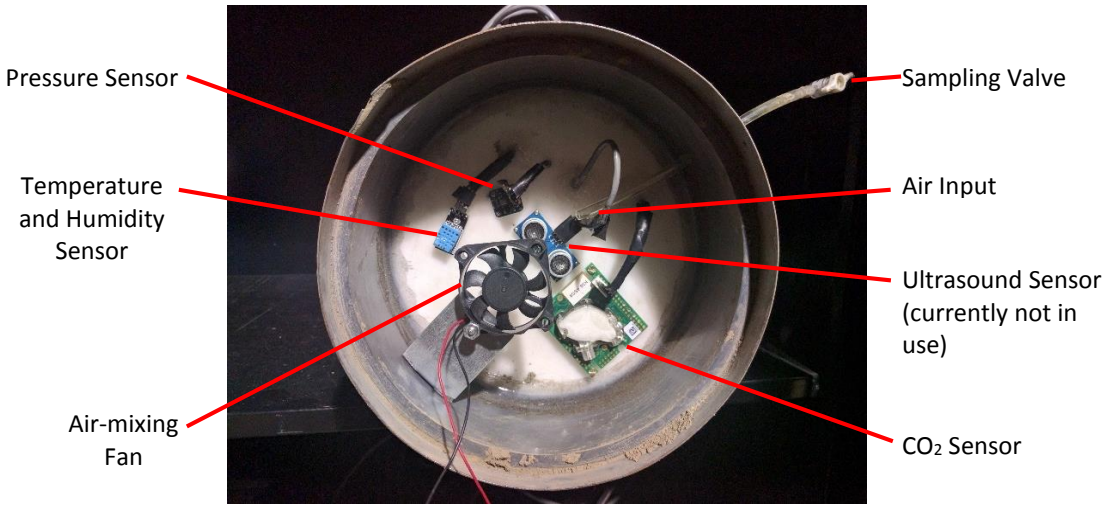

Figure 3.6: Bottom view, position of sensors and sampling tube

The CO_2 Engine K30 sensor used in the device is a low cost commercial unit (under $100) which does not require calibration due to the inclusion of the integrated ABC algorithm which accounts for long-term drift (SenseAir, 2012). NDIR (nondispersive infrared) CO_2 sensors such as the K30 work by emitting infrared light inside a tube

open to the air. The tube is plated by reflective material to ensure that all the emitted light reaches the other side where it will pass through optical filters before being read by two IR detectors (thermopiles). The reference thermopile monitors the intensity of light passed through a 4-μm center wavelength bandpass optical filter while the other measures the IR absorption through a 4.26-μm optical bandpass filter. The reference signal is used to monitor background interferences and obtain a cleaner signal (Wang et al., 2005). This setup can be seen in Figure 3.7.

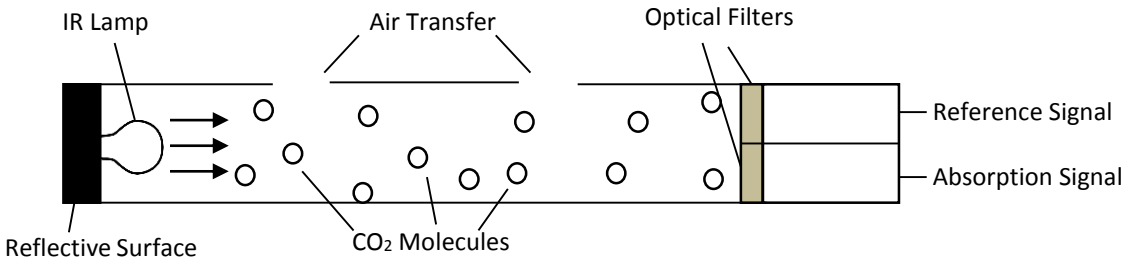

Figure 3.7: Components of an NDIR CO_2 sensor

NDIR devices work from the principle that CO_2 molecules will only absorb specific wavelengths of the IR light, letting all other wavelengths pass. The light is then filtered at the end of the tube to let only the said wavelength pass. The reading by the detector will therefore be the emitted light minus the absorbed light, hence, providing an indication of the concentration of the target molecule in the chamber (CO_2 in this case). CO_2 is known to absorb IR light at wavelengths of 2.7 μm, 4.3 μm and 15 μm. The 4.3 μm region is usually preferred, as in the K30 sensor, due to the maximum absorption and minimum interference on this band (Skoog et al., 1998). As explained by Sun et al. (2011) the spectrum of H_2O only slightly overlaps with CO_2 at 4.84 μm, (0.3%). While the manufacturers of the K30 sensor provide calibration equations for

temperature and pressure, humidity is not included. As such the effect of humidity on the CO_2 readings will be disregarded in these experiments.

3.1.3 Data Collection Protocol

The RSCA is self-contained and requires no preparation except for checking its power source. Once in the field, the RSCA is carried to the point of interest, pre-determined or not, and switched on at its main power switch. The ground cover of the location should be cleared of any detritus cover and ideally, lacking plants. If small plants are present, it is recommended to cut them as close to the ground as possible. While vegetation should not affect the respiration over such a short time frame, longer plants within the headspace could potentially hinder the air intake or interfere with the sensors. Residues covering the soil also should not directly affect the CO_2 concentration in the headspace but could be thick enough to cover up the soil surface and prevent proper extraction of the soil air. Sampling with the RSCA can be considered to consist of a pre-sampling, sampling and post-sampling period. The pre-sampling phase involves waiting roughly one minute for the sensors to normalize to atmospheric conditions after powering on the device. Then, insert the cutting blade fully into the soil, effectively sealing the headspace from the exterior air. This should be done with minimal disruption to the soil itself.

The sampling phase can then begin by a press of the logging button on the ECU, causing the LED on the device to start flashing, indicating to the user that the sampling period has started. The LED will flash once every time a sample is taken, hence, any

anomaly will be an indication to the user of a potential malfunction. The sampling period will last 150 seconds; the first 20 seconds used to record the CO_2 concentration in the air at the start of the sampling period so as to obtain a baseline. The sampling is performed at 1 Hz during the first 12 seconds when the GPS is recorded and at 5 Hz during the rest of the trial. As the RSCA position is static for the entire run, there is no need to continuously record positional data. Such a high sampling rate is unimportant for both the humidity/pressure DHT11 as well as the CO_2 Engine K30 sensor as their sampling rate is only 0.5 Hz. However, it is important due to the BMP180 pressure sensor which can be read at this speed and is used to detect a quick drop in pressure caused by the creation of negative pressure inside the headspace, before the soil air rushes in to replace it. This drop in pressure over atmospheric baseline can potentially be an indicator of the combined effect of soil porosity, texture and humidity. After 20 seconds from the start of the run, the pump will activate, vacuuming air from the chamber for four (4) seconds, then turning off again. This will have extracted the ambient air in the chamber and created a negative pressure, sucking air from the soil surface. The air being drawn into the chamber originates from an unknown volume of the soil matrix. This will be reflected in the drop in pressure created inside the chamber, as, if less air is drawn for the same vacuuming time, the pressure in the chamber will drop further then if more air had been vacuumed. This giving a strong hint as to the soil aeration. Once the pump is shut off, the pathway through it is not blocked, creating a way of normalising the pressure inside the device back to atmospheric level. The RSCA will then keep recording data

until the end of the sampling time, indicating the end to the user by turning off the LED entirely.

For the post-sampling period, the user is to remove the chamber from the soil and clean off any leftover soil from the cutting blade in order not to contaminate the next sampling site. Before moving on to the next point, the K30 will take roughly a minute to go back to ambient air concentrations. A flow chart of the Arduino code for the sampling process performed by the RSCA can be seen in Figure 3.8. Once all the points have been sampled, the user can simply remove the SD card from the ECU and transfer the data onto a computer.

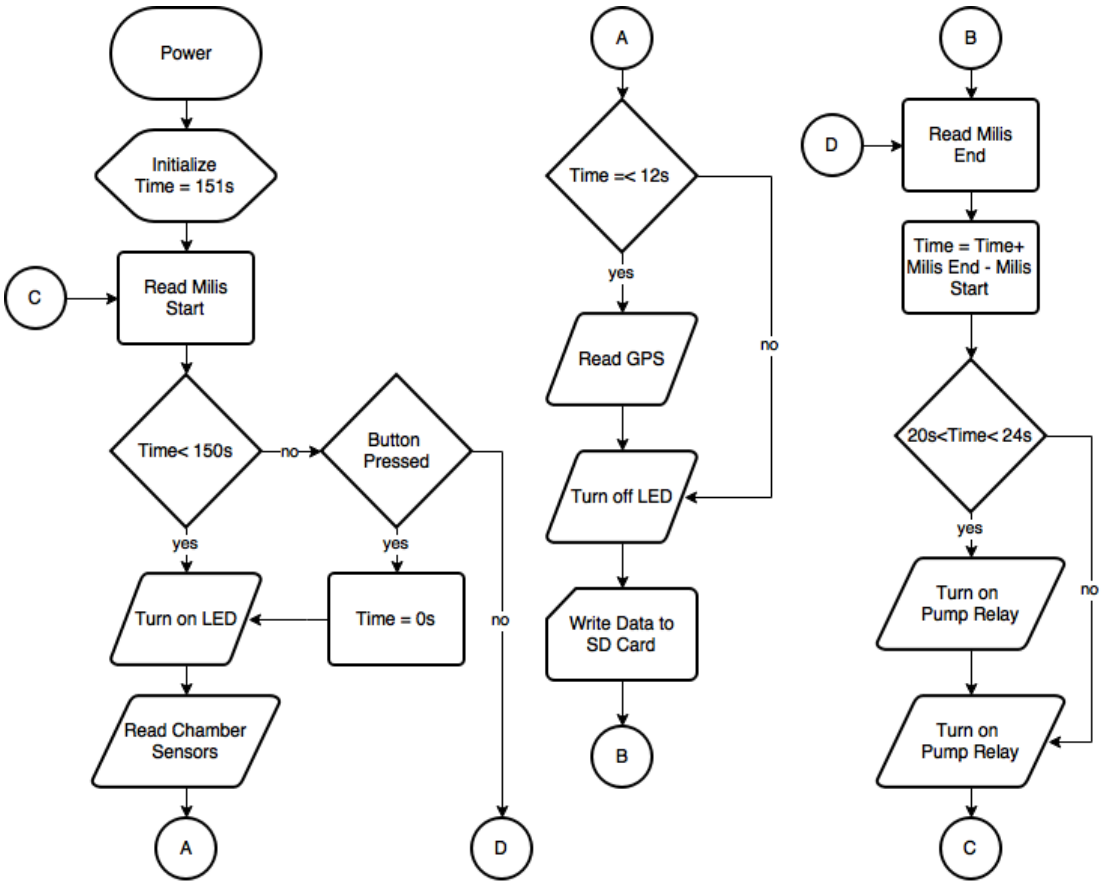

Figure 3.8: Flowchart of the Arduino Uno code for sampling process

3.1.4 Data Processing

The RSCA data is extracted directly through the on-board micro SD card. The data is output to a .txt file which is then processed through an in-house MATLAB® code. The first part of the code serves to filter the data, removing the data points higher than the CO_2 sensor range (10,000 ppm) or less than ambient concentration (~300 ppm, low estimate). The raw data is then separated by location and trial for ease of processing. Each trial produces around 750 points of data. Out of each trial, the points deemed important, such as the mean, maximum and minimum pressures, temperatures, concentration, are singled out and extracted for data modeling and any other statistical test. This data is then summarized and output for the user. The second part of the data processing comes in the form of a nonlinear regression performed in a separate Python™ code but run within the main MATLAB® script. In ideal conditions, the CO_2 Engine K30 sensor outputs data in the form of a curvilinear relationship with time following a first order response, as can be seen in Yasuda et al. (2012). As such the model for the curve can be written as follows:

$$C_t = C_{ss}\left[1 - e^{-\tau(t-\alpha)}\right] \quad (1)$$

where C_t = Measured concentration at time t in ppm, C_{ss} = Concentration at equilibrium in ppm, τ = time constant in s^{-1}, t = time in s and α = sensor offset in s.

For the code to work on a clean curve, the data is cut at the point of the lowest recorded pressure, as it coincides with the pump working at full capacity and indicates when the concentration starts to increase drastically. The data is also normalised to 0 for both time and concentration. Figures 3.9 and 3.11 show a typical

data processing sequence for a 24 trial day collected on Field 26 on October 12, 2015. Figure 3.10 shows a typical data curve both before and after the trim and normalisation.

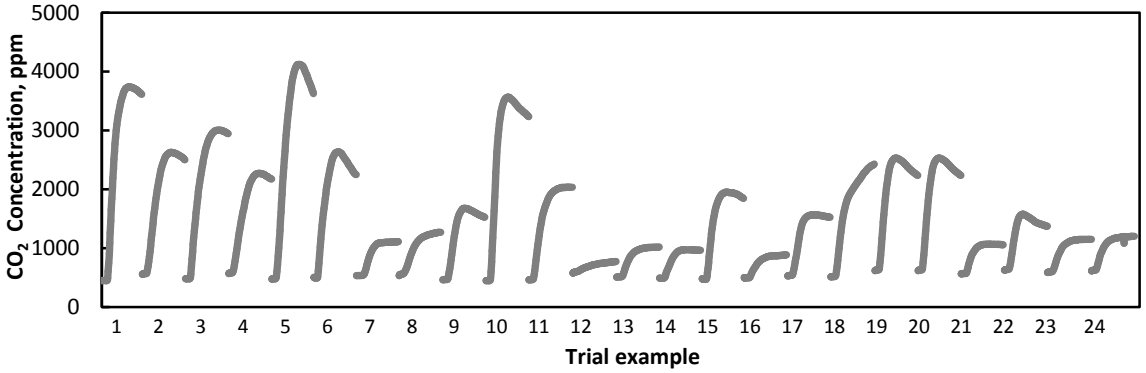

Figure 3.9: Sensor response curves from the all 24 trials of collected on Oct 12, 2015 at the Field 26 site

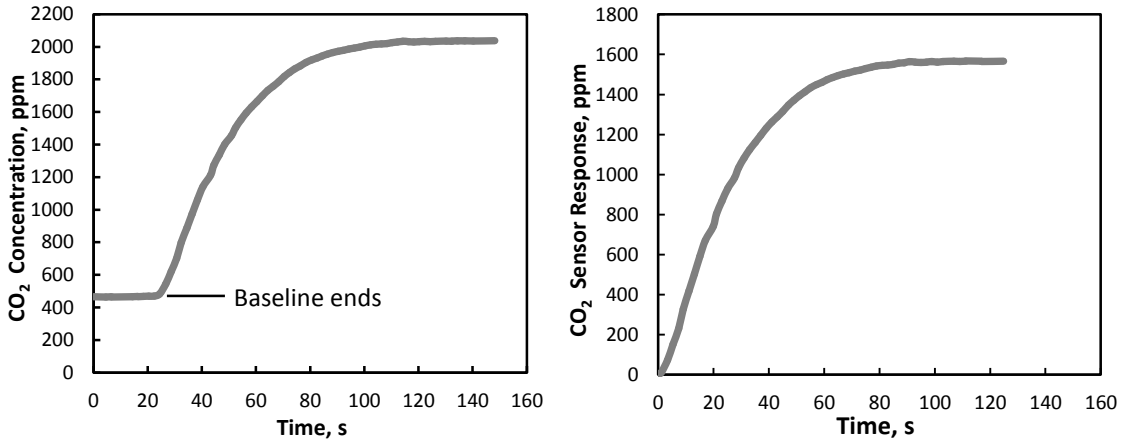

Figure 3.10: Concentration curve from the 11th trial of the data collected on Oct 12, 2015 at the Field 26 site shown as raw data (left) and as the concentration change with respect to the baseline (right)

The model is then fit to each individual curve in an attempt to find its parameters. Such a curve fitting can be seen in Figure 3.11. The need for this nonlinear regression arises from a number of the curves being incomplete due to taking longer than the sampling time to reach the steady state. All the parameters for the trial are consolidated and outputted into the summary sheet once again. These, along with the

previous ones, will be used when attempting to create a model or to run other statistical tests on the data.

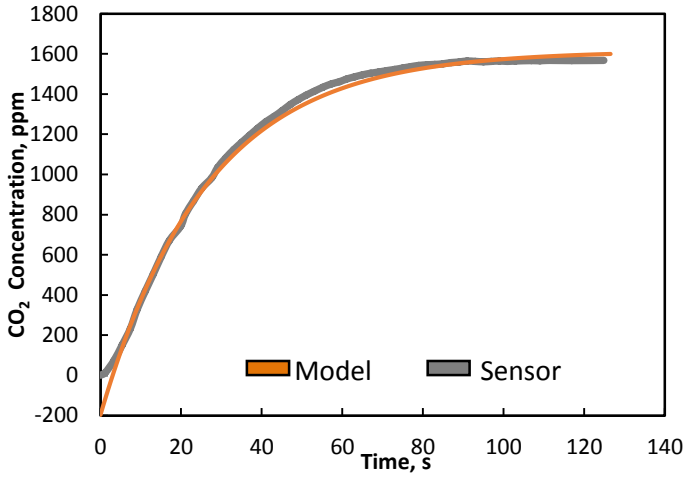

Figure 3.11: Recorded sensor measurement (grey) and model fit (orange) for the 12th trial of the data collected on Nov 12, 2015 at the Sherrington site

3.2 Sensor Testing

3.2.1 Introduction

The CO_2 Engine K30 sensor used in this experiment is central to obtaining reliable results. As such, before drawing conclusions from its readings, the sensor was tested for its accuracy. In addition, the mass of data obtained from regular use of the chamber, detailed in sections 3.3 Field testing and 3.4 Controlled experiment, were used to obtain an estimate of the sensor's time constant; this is a very relevant parameter to the RSCA's operating principle.

3.2.2 Experimental Setup

This experiment was run alongside the normal sampling procedure of the RSCA. During the normal 150-s sampling cycle the chamber is sampled three (3) times at set

intervals. The sampling was originally performed by inserting a sampling tube under the cutting disk during a trial. The final version of the chamber includes a built-in sampling tube, as can be seen in Figure 3.6. This change was done to avoid any potential leakage. During the procedure, the air is sampled using a syringe at 0 s, 45 s, and 150 s and injected into pre-vacuumed exetainers. These times were chosen as they represent the start and end of a trial as well as an arbitrary point in time 25 seconds after the start of the pump. The intermediary time was decided after initial experiments as a mid-response point between the two stable portions of the curve. These exetainers are then sent to the lab for analysis in a gas chromatograph. This experiment was repeated twice during the lifespan of the current chamber version. The first time was performed under field conditions during the experiment detailed in section 3.3 Field Testing. The samples were taken on Oct 12, 2015 at the Field 26 site (data for that field is shown in Figure 3.9). Sixteen out of the 24 trials were tested for a total of 48 samples plus ambients sent to the lab. The second repeat was performed during the experiment detailed in in section 3.4 Controlled Experiment which was performed in a controlled environment and hence, more homogenous soil. In this experiment, 12 RSCA trials were tested, spread equally among the various treatments for a total of 36 samples plus ambients, sent to the lab for analysis. The first set of samples were taken in a version of the chamber that did not include the air mixing fan; the second set did.

3.2.3 Statistical Analysis

The statistical tests were performed using the SAS software (SAS Institute Inc., Cary, NC, USA). The aim of the sensor validation procedure is to prove that, at the same point in time during a run, the CO_2 Engine K30 sensor records similar concentration values as the lab-analyzed sample. The desired result would be no difference in the mean of both populations. As such, the null and alternative hypotheses were stated as follows, where t_1, t_2, t_3 represent the 0, 45, and 150 s time points in the sampling run:

$$H_0: \mu_{1,t} - \mu_{2,t} = 0 \ (t = t_1, t_2, t_3) \quad (2)$$

$$H_1 : \mu_{1,t} - \mu_{2,t} \neq 0 \ (t = t_1, t_2, t_3) \quad (3)$$

Similarly, one can test for the similarity of the data points over all the times combined. The simplified hypothesis can be stated as follows:

$$H_0: \mu_1 - \mu_2 = 0 \quad (4)$$

$$H_0: \mu_1 - \mu_2 \neq 0 \quad (5)$$

Finally, it is possible to check for significance of the between (effect of the method type) and within (effect of time and time x method) subject effects. In SAS, this was performed by following PROC GLM (the General Linear Modeling procedure). The MANOVA and REPEATED statements are also called during the procedure. The CONTRAST option is also enabled to find significant differences of the measurement methods between the various times. The data sets for the field and controlled

experiments were processed separately. Additionally, the controlled experiment was split between the wet and dry treatments during processing.

3.3 Field Testing

3.3.1 Agricultural Greenhouse Gases Program

From 2013 to 2015, McGill University took part in the Agricultural Greenhouse Gas Program (AGGP). The stated aim of the entire project being to "provide Canadian farmers with technologies to manage their land and livestock in a way that will mitigate greenhouse gas (GHG) emissions" (Government of Canada, 2013). As part of the program, McGill University looked more specifically at the effects of irrigation and drainage practices on N_2O, CO_2 and CH_4, on both organic and mineral soils (Mat-Su, 2016). Within the scope of this study, closed static chambers (or non-steady-state non-flow-through chambers) were used to collect gases and calculate the soils respective fluxes. These chambers, while simple, were found to be unwieldy and time consuming and as such created the need for a faster, yet portable and low cost alternative. The Rapid Soil CO_2 Analyser (RSCA) described in this thesis was developed to this end.

While not all are published, some preliminary results of the AGGP have emerged. Fields Sherrington and St-Emmanuel have shown significant flux difference both between each other and temporally within each field, usually with peaks being associated with periods of spraying. As such, these fields were deemed suitable for

testing the experimental device discussed in this thesis. Field 26 of the Macdonald campus was added due to the high variation in soil types it contained.

The AGGP used the closed static chambers at eight different sites across Eastern Canada (Quebec, Ontario, Nova Scotia) from 2012 to 2015. Out of these, three (3) in close proximity to the city of Montreal were retained. At these sites, the RSCA was sampled alongside the classic chambers, hence, testing the prototype against an accepted method of soil respiration measurement. The aim of this study was the creation of a model using the sensor data obtained from the RSCA and correlating it with the results of the AGGP's static chambers at each location. Having been developed as a branching project and meant as an improved alternative to the static chambers in the field, the RSCA was tested in the same three fields.

3.3.2 Closed Steady State Chamber Design

The AGGP used closed static chambers (built by Casbo Plexiglass Inc. Montreal, QC, Canada) for all their field sampling. These chambers are considered inexpensive to produce and simple to use, hence, fitting the large scale of the project. The closed static chamber design is outlined alongside the RSCA in Figure 3.12. The main features of the chamber are: the base (or collar); the cover (or chamber), the cushion tape, the pressure equalizing opening and the sampling valve. The chamber base's dimensions are 0.556 x 0.566 x 0.140 m (W x L x H) and made of flexi-glass. The covers are 0.564 x 0.564 x 0.13 m (W x L x H) and covered in a layer of insulating aluminum to prevent sunlight from heating the chamber during the sampling period. The

cushion tape is installed on both the top of the base and the bottom of the cover to prevent air leaks. The lack of a locking mechanism means it must be manually adjusted *in situ*. The pressure equalizing opening is present to keep the interior air pressure at 1 atm and to let less CO_2 rich air escape; thus, this does not prevent air from the soil rising in the chamber. It consists of a simple opening on the top face of the cover prolonged by a coiling plastic tubing towards the inner chamber to prevent disturbance by external air movements. The sampling valve is fitted with a Teflon-silicon septa (National Scientific, Rockwood, TN, USA) to be sampled via a syringe. The overall cost for the closed static chamber system was approximately $100/unit ($35/base and $65/cover) while the reusable exetainers plus caps cost around $1350 per thousand units or $1.35/unit.

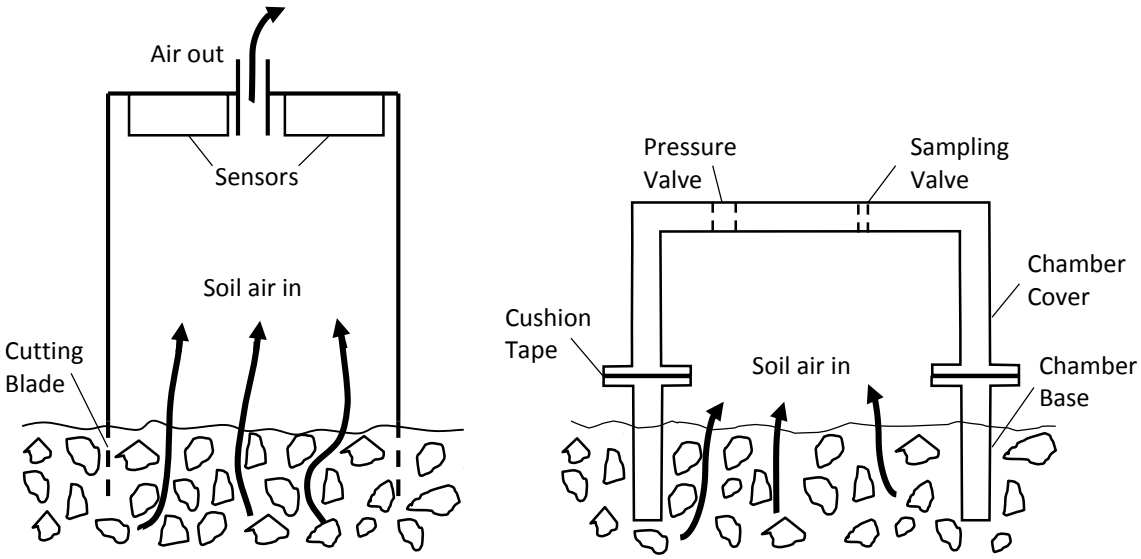

Figure 3.12: Side by side comparison of the working principles of the RSCA (left) and a classic, closed static chamber design (right)

3.3.3 Closed Steady State Chamber: Data Collection Protocol

The testing for the RSCA was performed at 3 sites across southern Quebec, all used during the AGGP. Each site had different soil characteristics and was used to grow different crops. Corn on sandy clay soils for the St-Emmanuel (SE) site, Onions on organic peat for the Sherrington (SH) site and soybeans on a loamy clay for Field 26 (F26), a field of Macdonald campus of McGill University. In order to test the RSCA's results, the device was sampled alongside (both temporally and spatially) the classic, closed static chamber design.

The sampling protocol using the closed static chambers is as follows. At the start of the sampling season, a collar is placed in the ground for each sampling location and kept there permanently until the season ends. The collar, or base, should be inserted in the soil at a set depth across the field and as equally as ground imperfections permit. In this experiment, the covers were inserted to protrude 10cm from the soil. All chamber bases were installed shortly after seeding and not directly on crops to avoid plants and soil movement from interfering with the gas measurement. Each sampling day, the chamber covers were carried onto the field and placed atop the base to seal it from exterior air. Samples were taken through the valve using a syringe at 0, 15, 30, 45, and 60 min, and kept in pre-vacuumed 12-ml exetainers (Labco, Wycombe, UK) fitted with a 60-mil (0.0625 in.) Teflon-silicon septa (National Scientific, Rockwood, TN, USA). These can be seen in Figure 3.13 alongside a chamber. The chambers were installed in various configurations and numbers at each of the three fields. Twelve single chambers in two rows were installed at the SE Site; 24

chambers in 3 groups of 8 were installed at the SH site; and 18 chambers in groups of 2 were installed at the F26 site. The exetainers containing the sampled air were then analyzed in the laboratory using a customized Bruker-Varian 450 gas chromatograph (Bruker, Bremen, Germany) using a Flame Ionization Detector (FID) and an Electron Capture Detector (ECD) to simultaneously measure CH_4, CO_2 and N_2O. The final result was the CO_2 concentration level in ppm for each of the exetainers, representing the five different time points for each of the chambers

Figure 3.13: Picture of non-steady state chamber and exetainers used for gas sampling, by Mat-Su (2016)

3.3.4 Closed Steady State Chamber Data Analysis

After sampling, the CO_2 concentration data for each sample is obtained from the lab. It is then processed through an in-house MATLAB® code created by Mat-Su (2016). Filtering was the first step via the creation of an upper and lower threshold. The former was created as a static threshold based on the minimum spectral detection of gas chromatography, namely 300 pm for CO_2, while the latter was a dynamic threshold based on previous (i-1) and subsequent samples (i+1). To activate the

dynamic threshold, a sample had to be both higher than 2.5 (empirical) times the previous value AND higher than the subsequent one. The filter can be summarised as follows:

$$(C_{v-CO_2})_i = \begin{cases} N/A & for \quad \left(C_{v-CO_2}\right)_i \leq 300\,ppm \vee \left(C_{v-CO_2}\right)_i \\ & \geq 2.5 * \left(C_{v-CO_2}\right)_{i-1} \wedge \left(C_{v-CO_2}\right)_i \geq \left(C_{v-CO_2}\right)_{i+1} \\ \left(C_{v-CO_2}\right)_i & for \quad Otherwise \end{cases} \quad (6)$$

Where C_{v-CO_2} = gas concentration in ppm and i = sample number. The data was also manually filtered for any erroneous values that could originate from either the sampling procedure or the handling of the gas during its analysis in the gas chromatograph. The next step was the conversion of the gas values from volumetric to mass basis (ppm to mg/m^3) using the following mass to volume equation from Holland et al. (1999)

$$C_m = \frac{(C_v * M * P)}{R * T} \quad (7)$$

Where C_m = gas concentration in mg m^{-3}, C_v = gas concentration in ppm, M = molecular weight of CO_2-C (12.0107 g mol^{-1}), P = atmospheric pressure (1atm), R= universal gas constant (0.0821 L atm K^{-1} mol^{-1}), and T= temperature (293K room temperature).

By replacing the known parameters this can be simplified to:

$$C_{m\,CO_2-C} = 0.5 * C_{v\,CO_2} \quad (8)$$

Where $C_{m\,CO_2-C}$ = gas concentration in mg.m^{-3} and $C_{v\,CO_2}$ = gas concentration in ppm. Flux can then be calculated through the concentration gradients over the duration of

the sampling. To take into consideration outlier data, a linear regression was applied between every possible permutation of two different measurements. This creates ten different slopes for the five samples that constitute a location. The median of the slopes is then used to calculate flux using equation (9):

$$f_t = V/A * Slope_{median} = H * Slope_{median} \quad (9)$$

Where f_t = hourly flux in mg m^{-2} h^{-1}, V = volume of the chamber in m^3, A = soil surface area covered by the chamber in m^3, $Slope_{median}$ = median of the ten calculated slopes in mg m^{-3} h^{-1}, f_t = h and H = height of the chamber measured from soil to top of the chamber cover in m.

3.3.6 Parallel Testing

During the summer of 2015, 12 days of simultaneous sampling with the classic chambers and the RSCA were recorded. Seven days at the SE site, four days at the SH site, and one at the F26 site. Sampling at the SE and SH sites was performed in parallel to weekly sampling with the classic chambers. For each static chamber point, two or more RSCA samples were gathered as replicates. The tests of the RSCA were performed within a 20-30 cm radius of the classic chambers locations, depending on field conditions. All of the sampling of the RSCA in the 2015 sampling season were performed using the third version of the device with the exception of the air mixing fan, which was added later. Previous testing had been performed in both 2013 and 2014, but due to drastic changes in chamber design, the data obtained from previous prototypes were incomparable to the sampling done in 2015.

On two different days, air samples from inside the RSCA chamber were gathered at the 0, 45 and 150-s marks. These samples were then sent for analysis in a gas chromatograph in a similar way to the sampling of the classic chambers. This was performed at 16 locations on a single day at the Field 26 site, with three time points at each for both the lab values and the sensor values. This data is the one used in section 3.2 Sensor Validation.

3.3.7 Comparative Modeling

The objective of this experiment was the creation of a model linking the flux data determined from the classic chambers with the sensor data obtained through the RSCA. The first step is the definition of the variables. In this case they will be as shown in Table 3.1 and extracted from the raw RSCA sensor data and the classic chamber data as described in section 3.1.4 and 3.3.4, respectively.

Table 3.1: Selected model parameters

Variables	Description	Origin
Flux	Calculated CO_2 flux	Classic chambers
ΔC	Steady state concentration - concentration at t=0 (from regression curve)	RSCA
H	Range of air humidity	RSCA
P	Baseline pressure - min pressure	RSCA
T	mean air temperature	RSCA
τ	Time constant	RSCA

These parameters and all potential interactions, were then used in an attempt to create a linear regression model under the classic form:

$$y = \beta_0 + \beta_1 X_1 + \beta_2 X_2 + \beta_3 X_1 X_2 + \varepsilon \quad (10)$$

Where $X_{1,2}$ are the variables that are included in the model (e.g.: Temperature, humidity, compaction as well as their interactions), β_0 is the intercept, $\beta_{1,2,3}$ are parameter estimates and ε is the error term. In SAS, the data was first modeled by site. Effectively attempting to create a model for each of the three sites separately from one another. Then by date, attempting to see if some days and different conditions would yield a more promising model. The PROC REG statement was used following a stepwise selection. Stepwise combines both forward and backward selection, methods as included variables may be then excluded and once excluded variables may be re-introduced into the model should they become significant. The slentry (or significance level) against which the p values were tested was tried at both 0.05 and 0.1 due to difficulty in obtaining any form of significance during the data processing.

3.4 Controlled Experiment

3.4.1 Introduction

As can be seen in section 4.2.2, the field experiment attempted during this project yielded unsatisfying results. The variability of data obtained in the field was difficult to explain. The results could originate from variations in temperature, humidity, micro-topography or even accidental human interventions. This spurred the need for an experiment performed in controlled conditions. According to the literature, temperature is the main factor affecting soil respiration. From the working principle of the chamber and the field experience, soil compaction is a factor affecting directly

the RSCA. As such, these two factors were chosen to create a 2 by 4 factorial experiment. Additionally, substrate induced respiration was added as a third factor by the addition of glucose to all existing treatments. The results were expected to show lower variability within a treatment than the field data but large differences between the treatments.

3.4.2 Experimental Setup

The experiment varied three factors deemed as having potentially strong effects on soil respiration. These were: compaction level, moisture level and the presence of glucose. While other factors such as temperature or organic matter content can be considered equally as important, they are also much harder to control when dealing with large amounts of soil exposed to the air (a requirement for the testing of the RSCA device). Additionally, as the aim of the experiment was to induce strong responses in the sensor data, only two levels of each factor were deemed necessary. They were a "detrimental" level, inhibiting soil respiration, and an "optimal" level where the factor is being adjusted to maximise soil respiration.

The experiment was set up as shown in Figure 3.14 Four large containers (~0.75 m^3) are filled with ~180 kg sandy loam (wet weight). The soil was taken from the A horizon of field 68, (Macdonald Campus, QC, Canada). This soil type is considered optimal for this experiment as it can be compacted, dried and wetted easily. Each of these containers held a different treatment, these being all possible factor

combinations: Dry/Compacted, Dry/Not Compacted, Wet/Compacted and Wet/Non Compacted.

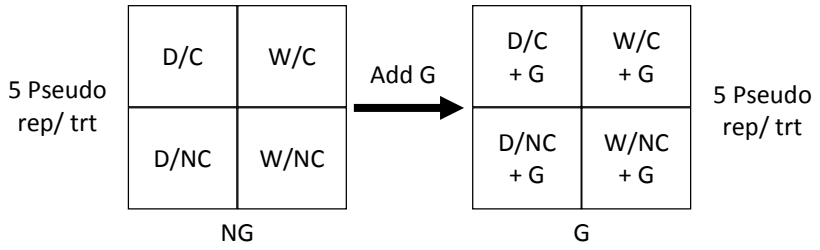

Figure 3.14: Proposed experimental setup where D is Dry, W is Wet, C is Compacted and NC is Non Compacted. G and NG represent respectively the presence of glucose and its absence

The values of these different factors are meant to either hinder or improve soil respiration. The soil was considered dry after being air dried for 48 hours under a sunny day, leaving it as close as possible to only the structural water. The soil was considered optimally wet at roughly 60-65% of its field capacity (or ~15-20% volumetric water content for a sandy loam soil). The compaction level of the soil was measured by its bulk density. The non-compacted soil was only lightly compacted in order not to leave any overly large and unnatural air gaps. The compacted soils on the other hand were compressed into the containers, layer by layer, by pressing equally on their surface with heavy loads. The exact bulk density and volumetric water content of the soil each day of the experiment can be seen in Table 3.2.

Table 3.2: Data table showing the wet and dry bulk densities (BD) as well as the gravimetric and volumetric water contents (WC) of the various treatments on each day of the experiment

Date	Treatment	Wet BD (g/cm3)	Dry BD (g/cm3)	GWC (%)	VWC (%)
29-Jul-16	W/C	1.32	1.04	0.27	0.21
29-Jul-16	W/NC	1.22	0.97	0.27	0.21
29-Jul-16	D/C	1.13	1.10	0.03	0.03
29-Jul-16	D/NC	1.15	1.12	0.03	0.03
1-Aug-16	W/C	1.29	0.70	0.22	0.18
1-Aug-16	W/NC	1.22	0.64	0.22	0.18
2-Aug-16	W/C	1.50	0.78	0.36	0.26
2-Aug-16	W/NC	1.27	0.60	0.39	0.28
3-Aug-16	W/C	1.51	0.81	0.33	0.25
3-Aug-16	W/NC	1.27	0.60	0.40	0.29
3-Aug-16	D/C	1.20	0.75	0.02	0.02
3-Aug-16	D/NC	1.13	0.68	0.02	0.02
15-Jul-16	Field	1.57	1.13	0.40	0.28

All containers were stored in the same indoor area, and therefore, were under similar conditions, especially with regards to temperature shifts. Initially, no glucose was added to any of the original treatments. As can be seen in Table 3.2, different moisture levels of the "wet" moisture treatment were attempted to see their potential effects on soil respiration. These can simply be considered as low, medium and high. Inspired by the experiment from Kaur et al. (2015), glucose was added to all treatments once the previous sampling was complete. Glucose was chosen as substrate as most soil microorganisms can use it as a carbon source (Stotzky & Norman, 1961) and originated from Sigma-Aldrich Canada Co. (Oakville, ON, Canada). 180 g of D-(+)-Glucose at ≥99.5% purity was added to each treatment.

3.4.3 Data Collection

Each container/treatment was sampled 5 times per day. The soil in the containers was then stirred and shaken before being brought back to initial conditions and

sampled 5 times again the next day. The loose soil was only lightly leveled between each trial to avoid holes from the RSCA insertion. The “compacted” treatment soil on the other hand was compacted back down to original levels after each sampling run as the insertion and removal of the RSCA in compacted soils tended to break the top compacted layer. It had no effect bellow 5 cm.

Both treatments of the dry soil were only sampled one day (5 trials) without glucose and one day (5 trials) with glucose. This was done as the data clearly showed a very consistent lack of soil respiration in those soils and the treatment was not modified between the days. This added up to three days of data taken on each of the wet treatments without glucose and one on the dry treatments without glucose. Once the glucose was added, one more day of data was taken for each treatment. In parallel to the RSCA sampling, the device was manually sampled via the method explained in section 3.2.2 and the gas sent to the lab for analysis.

To know the exacts bulk density and water content of each treatment for each day of the experiment, soil was sampled using a core, 5 cm high and 4.35 cm ID. The soil was weighed wet, then dried in an over at 110°C for 24 h before being weighed again. A set portion of each soil sample was then burned in a furnace at 375°C for 16 h (overnight) to find the organic matter percentage in each treatment and over time. The results of these tests can be seen in Table 3.2.

3.4.4 Data Processing

The experiment yielded 60 RSCA trials for all days combined, each taking continuous measurements over three minutes at roughly 8 Hz for pressure, temperature and humidity, and 0.5 Hz for CO_2 concentration. The data were then observed for sensor responses that can be attributed to individual treatments. Dried and compacted soil was expected to show the lowest increase in CO_2 concentrations over the ambient values due to its poor support of microbial activity and lack of organic matter content. Additionally, soil under such treatment is expected to show clear dips in the pressure values inside the headspace as heavy compaction can prohibit air from seeping through the soil surface. This is compounded in the wet soil as water will decrease even further the aeration porosity of the soil, allowing for greater compaction. The wet and non-compacted soil was expected to show the highest level of CO_2 concentrations as it held optimal conditions, both for the microbial activity, but also for the air to easily seep out from the soil surface. Finally, adding glucose to every treatment was expected to multiply the concentration values obtained. As such, the soils with little to no microbial activity were still expected to show similarly low levels of concentrations, while the soils already showing healthy levels of CO_2 emanations would most likely see these increase even further.

The raw data obtained from the RSCA were processed as is outlined in section 3.1.4. Statistically, the treatments were first tested for the effect of soil moisture, compaction and soil moisture x compaction. This was performed as a 2 by 4 factorial with two (2) levels of compaction and four (4) of soil moisture. This processed via a

two-way ANOVA called by the PROC MIXED procedure in SAS. The data can then be displayed as LS Means and tested using the Tukey mean comparison method for any significant difference in treatment. Next, the effect of the substrate induced respiration was tested by checking the glucose supplied soils against the same treatment without glucose. Due to only having two moisture levels available for the glucose treatment, this was set up in a separate three-way ANOVA checking for the effect of soil moisture, soil compaction, glucose presence along with all their respective interaction effects.

Chapter 4 Results and Discussion

4.1 RSCA Development

4.1.1 Results and Discussion

As stated in section 1.3, the chamber's main design constraints were the portability of the chamber, its ease of use, its reliability and its accuracy, while maintaining low construction costs. The RSCA development spanned the better part of a year. The price of the individual components of the final design can be tallied up for an estimated price of the prototype chamber. Some components such as in-house 3D printed parts or small wiring were estimated and filed under miscellaneous as can be seen in table 4.1

Table 4.1: Price breakdown of the RSCA chamber by component

Component	Function	Manufacturer	Price, $CAD
Arduino Uno (rev 3)	Microcontroller	Arduino	$23.30
CO_2 Engine K30	CO_2 Sensor	SenseAir	$85.00
DHT 11	Temperature and Humidity Sensor	Adafruit	$5.00
BMP 180	Pressure Sensor	Adafruit	$9.95
Ultimate GPS shield	Positioning and Data logging	Adafruit	$44.95
Sensor Shield	Wiring	Generic Robotics	$5.91
DFR0017 Relay Module V2	Relay for Pump	DFRobot	$9.95
AP638 Electric Air Pump	Air vacuuming	Intex	$9.99
Fan-202-5V	Air mixing	Sparkfun	$5.95
1' of 8" PVC Pipe	Structural	N/A	$8.50
1.5" thick Delrin Plastic sheet	Structural	N/A	$150
Miscellaneous	Wires, batteries, 3D prints, etc.	N/A	~$100
Total			458.5

As can be seen in section 3.3.2, classic chambers cost $100 per chamber. These closed static chambers can only sample a single point in an hour (less with the use of a

commercial IRGA), in addition to the setup time, and need to be used in groups to be time efficient. Taking into account that a field in the AGGP study required approximately 12 chamber to be used at once in addition to hundreds of exetainers, the cost of such a setup is upwards of $1300. This does not include the additional labor which is not required to operate the RSCA. On the practical side, the RSCA weighs in at 4kg making it easily portable in the field. With only a single button to press and the data logging to a simple SD card, the RSCA is also easy to use. While it cannot be used with tall vegetation or in the presence of overly thick residue on the soil surface layer, this is a common drawback of most chamber systems. The system can still be used with light vegetation such as grass.

The first order response modeling described in section 3.1.4 was used on eleven data sets from the field experiment (section 3.3) as well as the controlled experiment (section 3.4). The MATLAB® portion alone was used for the sensor validation (section 3.2). The modeling was robust and rejected very few of the input data sets. The rejected ones were usually due to errors in sampling along with unrecoverable or incomplete data sets. While the specific use of these results is discussed in section 4.2, 4.3 and 4.4, both the time constant and offset time's average were calculated for all data sets combined. The average time constant of the CO_2 Engine K30 sensor was $0.0317 \pm 0.0045\ s^{-1}$ while the offset time due to the permeable membrane of the sensor was 4.23±0.85 s. This falls in line with previous research done on the sensor (Yasuda et al., 2012) which reported a time constant of between $0.045 \pm 0.026\ s^{-1}$ after 37 days

of use and 0.024±0.004 s^{-1} after 306 days. The respective offsets were 6.1±1.8 s and 4.8±2.6 s.

4.1.2 Design Improvements

A number of enhancements could be made to the chamber. The main issue encountered during sampling was the resilience of various soil textures to the cutting blade on the bottom of the device. While the blade performed adequately in loamy soils, both extremes of aerated organic soils and heavy clay soils caused sampling issues. The former soil type would let the chamber sink past the blade, hence, reducing the total headspace of the chamber. Such an aerated soil with high pore connectivity could also potentially be letting ambient air seep back into the chamber during vacuuming. The clay soils caused the opposite issue of hindering the insertion of the cutting disk through the soil surface. In the common case of uneven terrain, a non-complete insertion of the blade on one side of the chamber could cause leakage on the other. The solution to such an issue would be the potential addition of a spring loaded blade, doubled with a stopper on the perimeter of the chamber to prevent it from sinking too far in soft aerated soils. Other, more minor improvements, could be made to the RSCA, including the addition of an air flow sensor to monitor exactly the input of air from the headspace to the pump. This could then be checked in parallel to the pressure sensor for a better understanding of the events in the headspace.

4.2 Sensor Testing

4.2.1 Results

The results of the sensor validation tests from Field 26 and from the controlled experiment can be seen in Figure 4.1 and 4.3, respectively. The data is displayed as box plots of the difference between the GC and RSCA methods. Hence, above the 0 line the GC recorded higher CO_2 concentration at a point in time, while bellow means the K30 sensor was in turn higher. The runs have been separated by time to illustrate the disparity of the two methods at the same time point during each trial. Figure 4.3 additionally distinguishes between the two different moisture treatments (wet and dry). Each box is constituted of 16 and 6 trials in Figures 4.1 and 4.3 respectively.

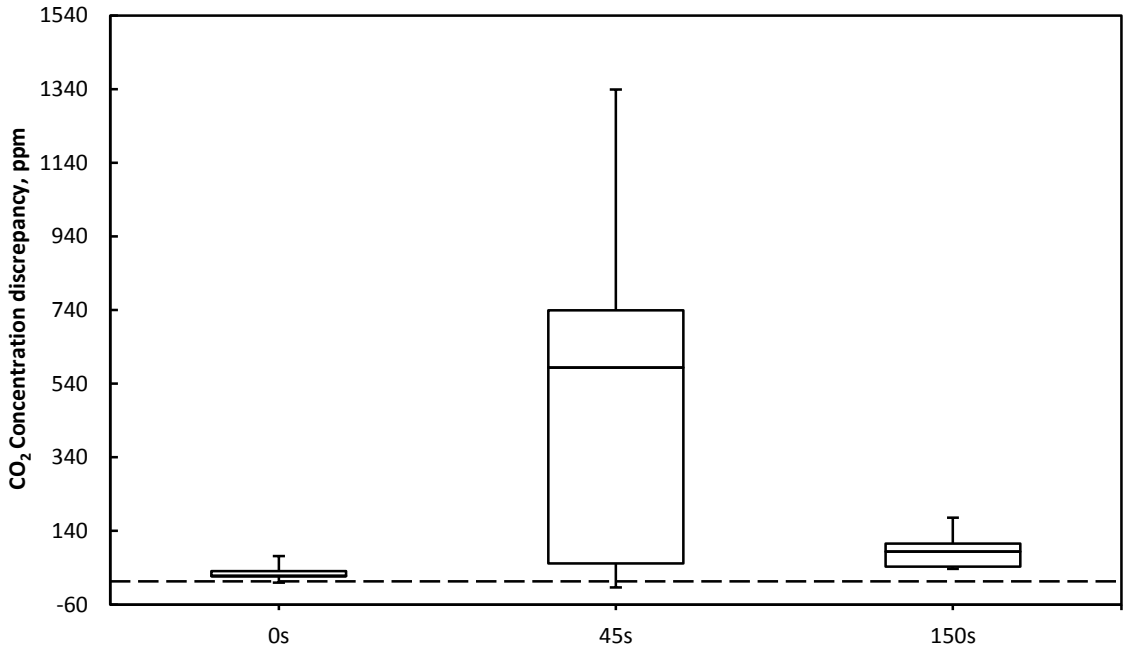

Figure 4.1: Box plot of the difference in CO_2 concentrations measurements of both measurement methods (GC and RSCA) at three time points (0, 45, and 150s) through sampling of 16 locations on a single day at the Field 26 location

Some location's measurements never reached above 1000ppm at any of the three-time point for either measurement method. In such cases the gas increase inside the chamber is likely slower than at the other locations and as such would not suffer from the same sensor issues as the other trials. Removing these points from the data to isolate the sets featuring maximum concentrations of >1000ppm results in Figure 4.2.

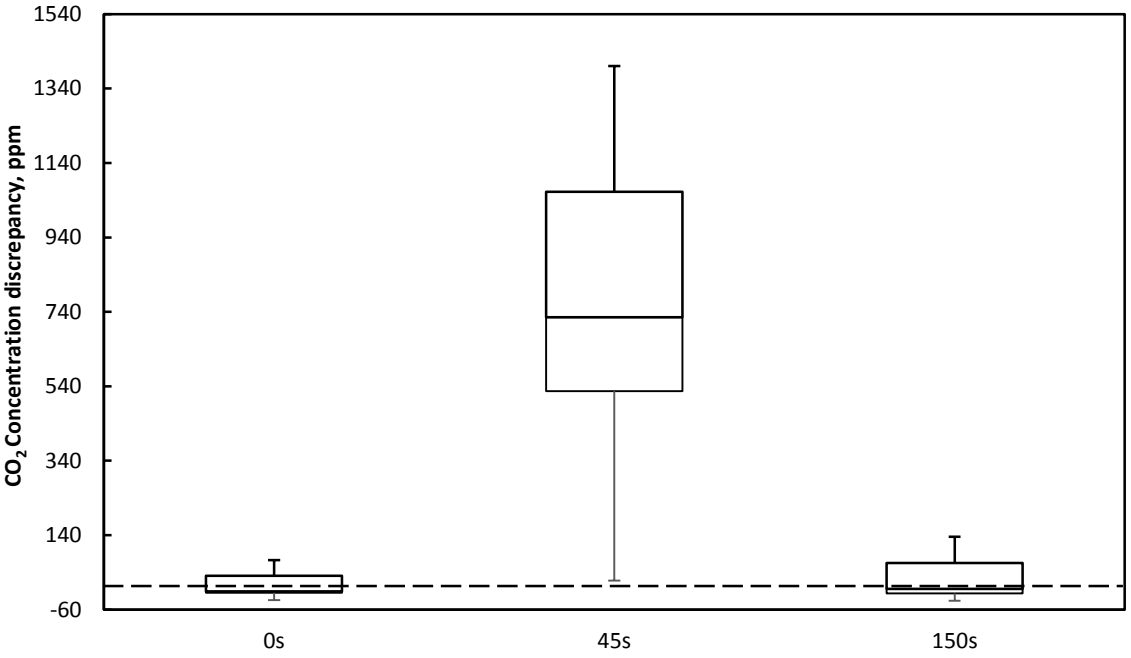

Figure 4.2: Box plot of the difference in CO_2 concentrations measurements of both measurement methods (RSCA and gas chromatograph) at three time points (0, 45, and 150s) for the through sampling of 16 locations on a single day at the Field 26 location

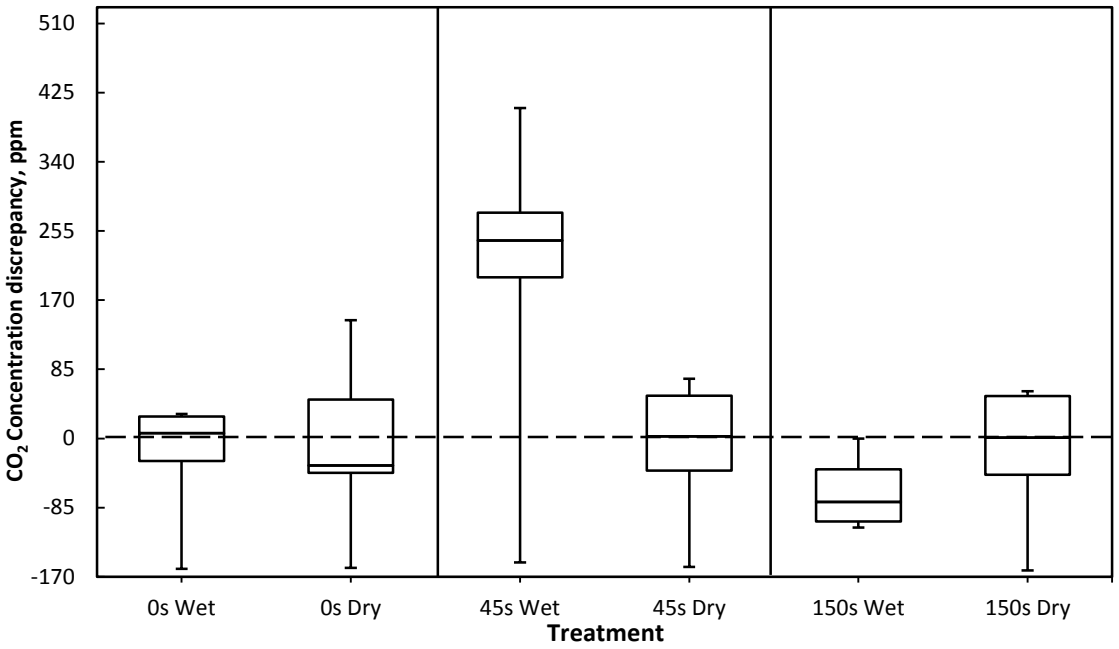

Figure 4.3: CO_2 concentrations of both measurement methods (RSCA and gas chromatograph) at three time points (0, 45, and 150s) through sampling of both the wet and dry treatments of the controlled experiment

Figure 4.1 and 4.3 both show higher readings from the gas chromatograph as opposed to the K30 CO_2 sensor at the 45 s mark. All other plots, with the exception of the 150 s Wet in Figure 4.3 which trends slightly in the opposite direction, hover around a null difference at their median. Figure 4.2 serves to visually exacerbate this difference when isolating the trials that rose above 1000ppm CO_2. Figure 4.3 further supports this trend as the 45 s Dry plot fails to show any similar differences as the 45 s Wet. This can be explained by the Dry samples never reaching the high CO_2 concentrations needed to expose this discrepancy. The statistical analysis introduced in section 3.2 supports the visual indications.

For the first hypothesis looking at each time point individually, we failed to reject the null hypothesis for time 0s and 150s ($p>0.05$) while we rejected it at time 45s. For the

second hypothesis, looking at all times combined and from the MANOVA statement results, looking specifically at the Wilk's lambda statistical test, we rejected the null hypothesis for the effect of the measurement method on the concentration for all times combined ($p<0.005$). Finally, the effect of time and time by method are found to be significant at $p>0.05$. The CONTRAST option also follows along the same lines, showing differences in the results of the method between time 0s and 45s but not between 0s and 150s. These findings hold true for both the field and the wet treatments in the controlled experiment. The dry treatments were found to demonstrate no significant differences at any time with the GC values.

While the CO_2 Engine K30 sensor follows a first order response, the actual increase in CO_2 concentration shows a fast original increase before leveling off steeply once the gas has fully filled the chamber. Due to the steepness of this increase, the K30 reacts similarly than as to a step input. While unable to directly record this, it can be visually illustrated by plotting a simple time series of both methods under the wet treatment, as can be seen in Figure 4.4. Observing the plot of the GC method hints at the aforementioned steep increase. As there are no samples between 0s and 45s, it is impossible to tell from this data the true accumulation rate of the CO_2 inside the chamber.

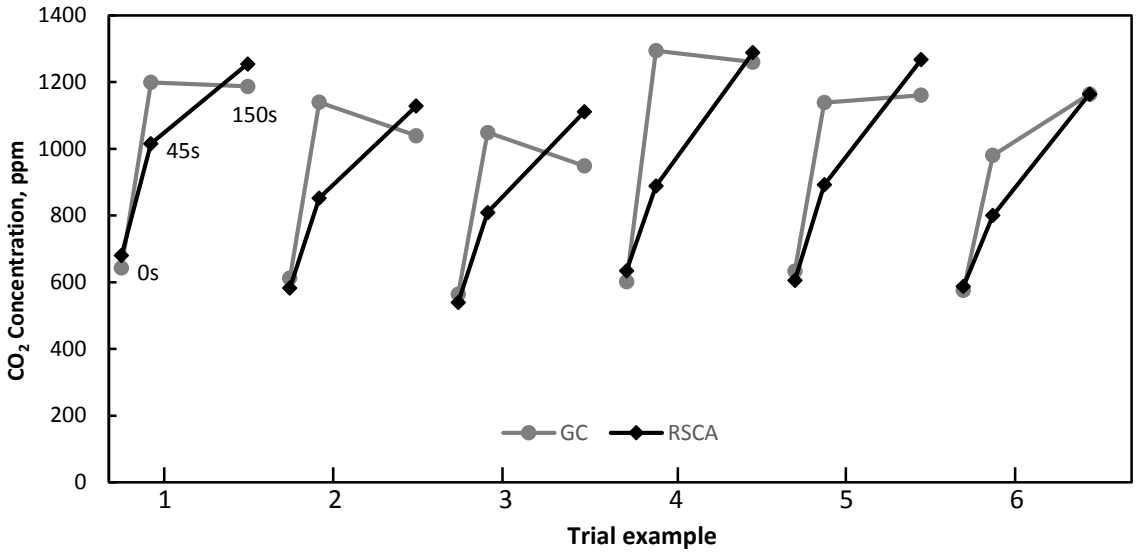

Figure 4.4: Time series of the CO_2 concentrations of both measurement methods (RSCA and gas chromatograph) at three time points (0, 45, and 150s) for 6 trials in lab conditions

4.1.2 Discussion

The validation of the on-board CO_2 sensor by comparing its results with the lab tested values yielded very clear results. The natural step input of the gas being very steep, the sensor was unable to follow as quickly (time constant > 30 s) and, following a first order response, left a significantly large difference in values between it and the GC results during the sudden increase around the 30-50 s mark (Figure 4.4). This issue did not allow the use of the gradient of the linear portion of the curve as a reliable variable for the model creation, as it was dictated by the time constant of the sensor and not the actual concentration increase. During the stable portions of the trial, both before creating the negative pressure and if the steady state was reached, the values were significantly close to the ones tested by gas chromatography in laboratory. This shows the CO_2 Engine K30 sensor as adequate for recoding in stable systems and where the increase rate is lower then it's time constant allows.

The first order response modeling was devised as an alternative to using the slope of the gas concentration increase. This test was important in determining the factors to be used in the modeling section of the field experiment (section 3.3) as well as the ones to examine for changes in the controlled experiment (section 3.4). Improvements to the sensor could be made such as an upgrade to the K-30 FR (fast response) 2 Hz, CO2 Sensor (CO2Meter, Inc., Ormond Beach, FL, USA). The increased sampling rate being useful in a rapidly changing system. The sensors both note a 20 s diffusion time as part of their response time required to reach the actual value; however, switching to the K-30 FR would more than double the price of the sensor.

4.2 Field Experiment

4.2.1 Results

The goal of this section is the creation of a model relating the RSCA data to the flux obtained from the closed static chambers. The first attempt was done using the individual model parameters listed in Table 3.1. This yielded no conclusive results as is exemplified in Figure 4.5. The strongest correlation found was with temperature, at $R^2 = 0.37$; however, it is still extremely weak.

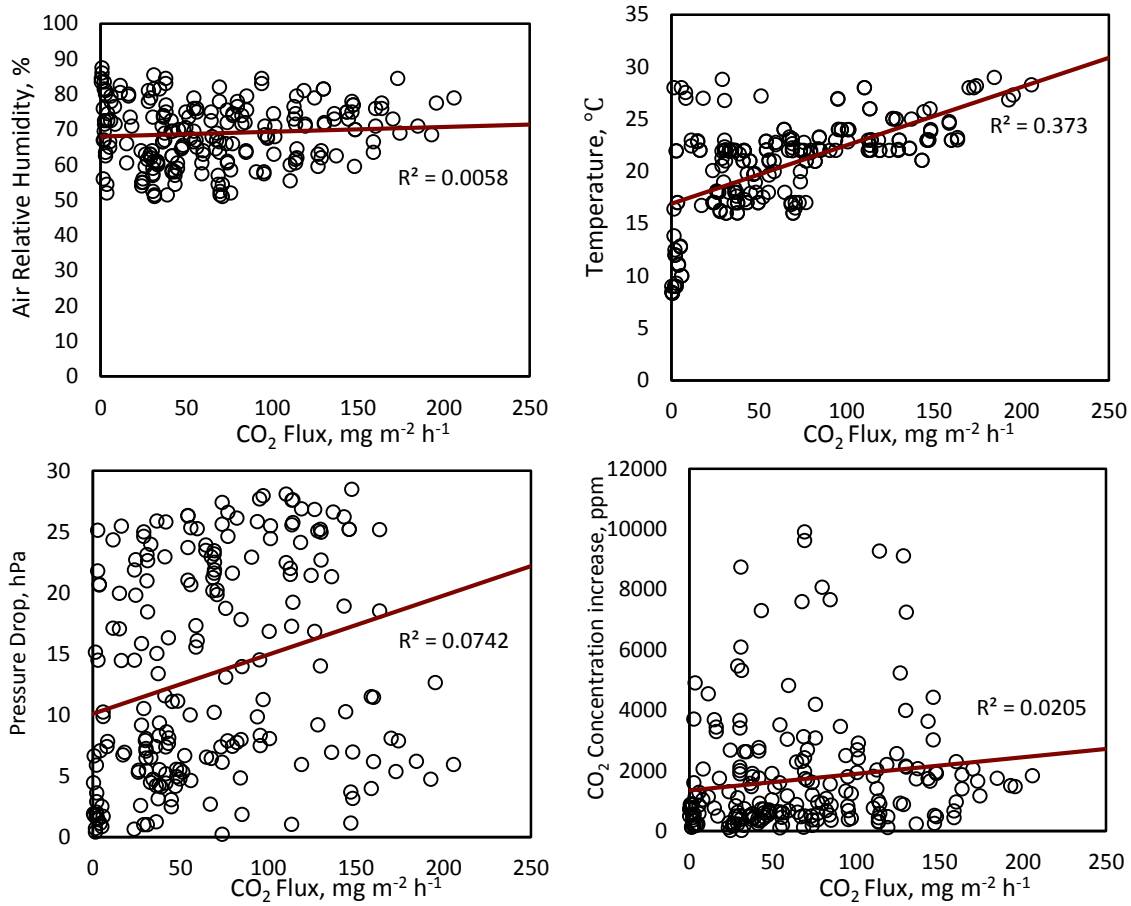

Figure 4.5: Correlation between humidity (top left), temperature (top right), pressure drop (bottom left), and CO_2 concentration change (bottom right) and the closed static chamber flux

Running the SAS code for the model creation yielded the results given in Table 4.2. The software was run individually by site and for all sites combined. All variables, both main effects and interactions, that were entered and kept in the model using the stepwise selection, were recorded along with the R^2, adjusted R^2 and RMSE for each site.

Table 4.2: Result of the unmodified linear regression modeling showing only included variables and their respective parameter estimate. The R^2, adjusted R^2 and RMSE of each model are also shown.

Site	R^2	Adj. R^2	RMSE	Variable Entered	Parameter Estimate
Combined	0.402	0.393	39.13	Intercept	-111.35 ± 25.57
				Humidity	0.66 ± 0.31
				Temperature	7.04 ± 0.6
				Time constant x Temperature	-22.2 ± 9.85
SE	0.49	0.48	35.98	Intercept	-75.97 ± 13.03
				Temperature	7.39 ± 0.63
				Time constant x ΔC	-0.102 ± 0.05
SH	0.302	0.283	51.662	Intercept	19.75 ± 13.88
				Time constant x ΔC	1.36 ± 0.36
F26	0.24	0.21	11.52	Intercept	192.3 ± 57
				Temperature x Humidity	-0.12 ± 0.045

The results for the final model for all sites combined can be seen in Figure 4.6.

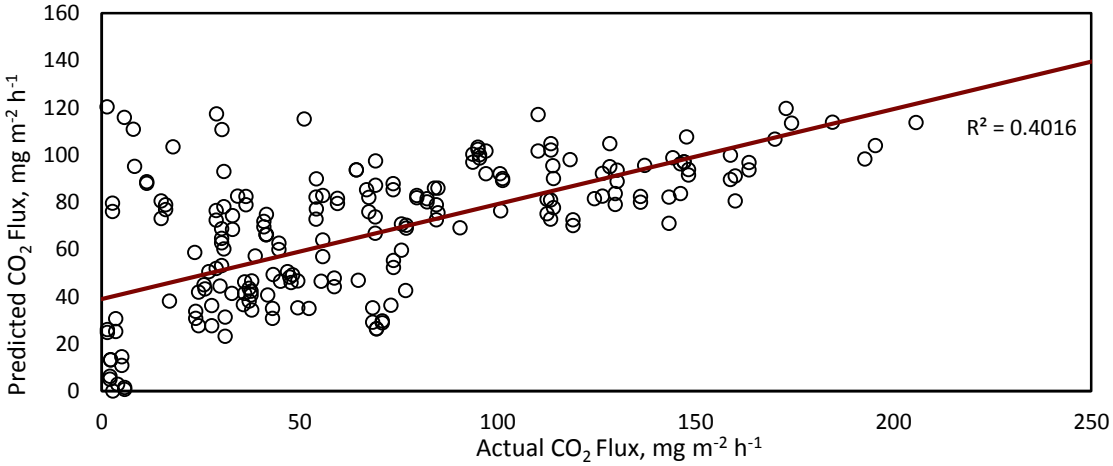

Figure 4.6: Scatter plot of the predicted vs the actual flux values, showing the trendline and R^2 for the unmodified model of all sites combined

The relationship at high actual fluxes tends towards linearity but deteriorates at the low fluxes where some predictions are found to be excessively high. As the fit of the model is not ideal at $R^2 = 0.40$, a potential improvement comes from looking at the residual vs predicted values graph seen in Figure 4.7 (top). The data in this figure

shows heteroscedasticity, suggesting a simple straight line is inappropriate as a model. As recommended by Fernandez (1992), a natural log transformation was attempted on the data, both on the predictors and the response.

$$y' = \ln(y) \tag{14}$$

Where y = flux from the classic chambers and y' = transformed flux. Using y' as a base for a new model the second residual vs predicted plot of Figure 4.7 (bottom) was generated.

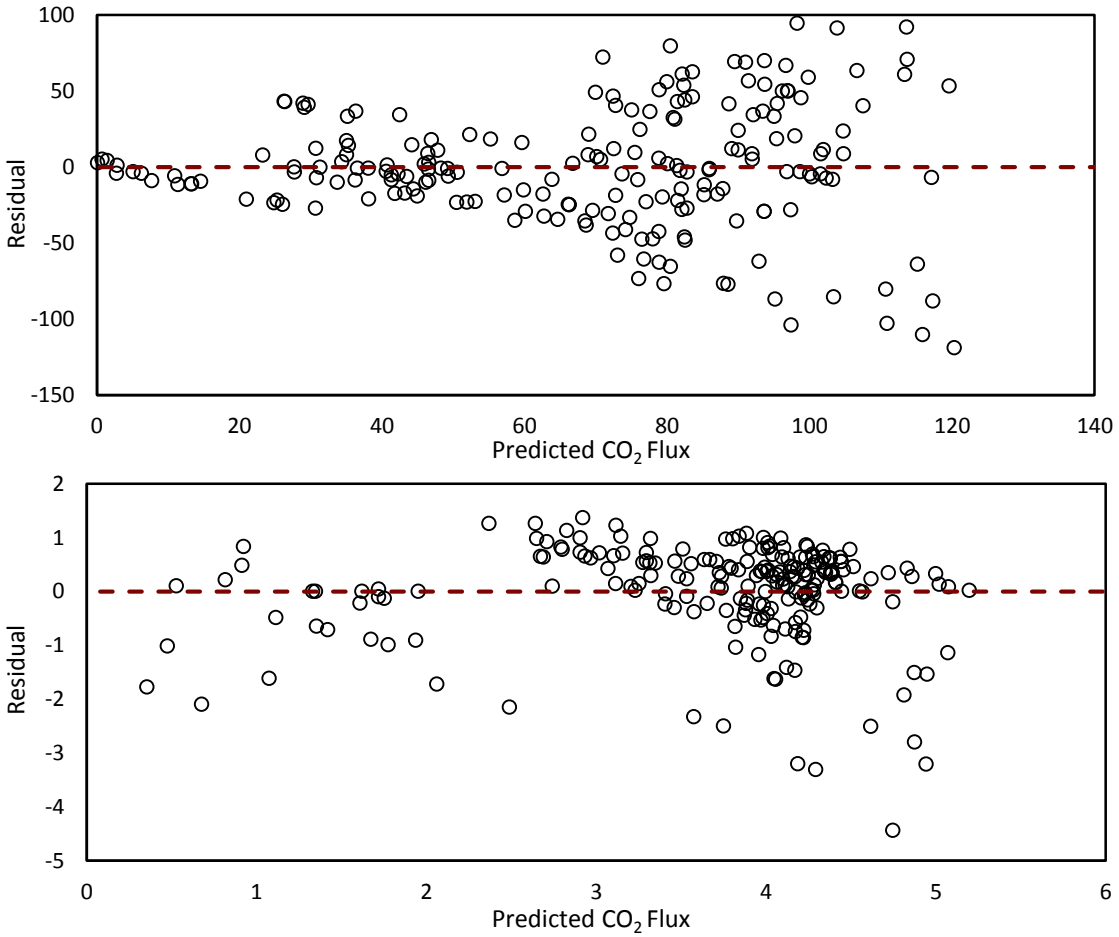

Figure 4.7: Predicted VS Residual scatter plot before (top) and after (bellow) transformation from y to y'

As can be seen from the four graphs in Figure 4.8, the fit was slightly improved for all main factors with respect to the flux of the classic chambers.

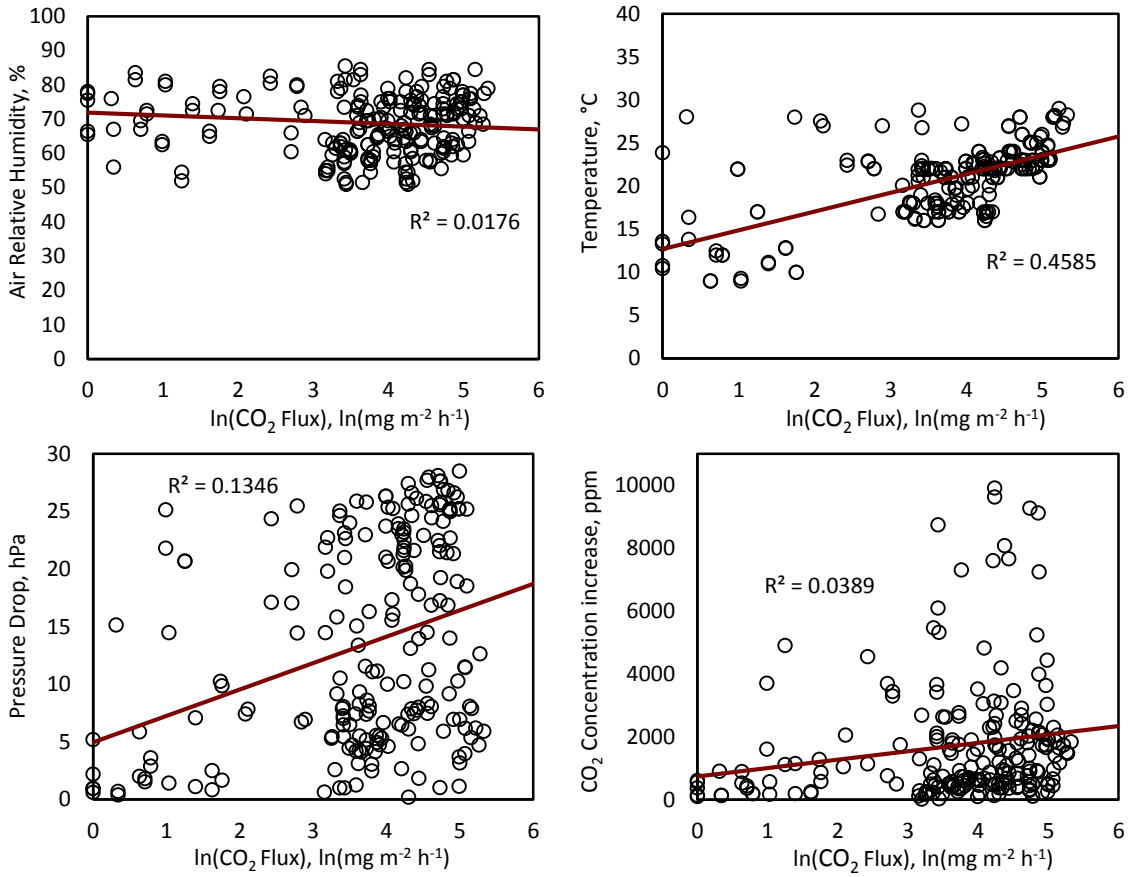

Figure 4.8: Correlation between humidity (top left), temperature (top right), pressure drop (bottom left), and CO_2 concentration change (bottom right) and the transformed closed static chamber flux

The effect of the transformation can also be seen in the overall model across all sites as is displayed in Figure 4.9:

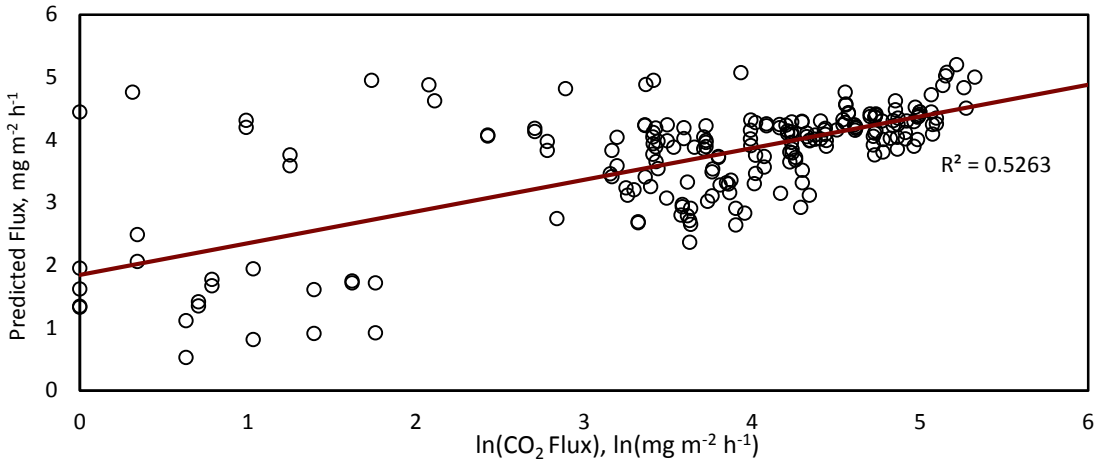

Figure 4.9: Scatter plot of the predicted vs the actual flux values, showing the trendline and R^2 for the model of all sites combined after natural log transformation of the response

The detailed result of the SAS code for all sites combined and individually can be seen in Table 4.3.

Table 4.3: Result of the linear regression modeling with ln(y) transformation, showing only included variables

Site	R^2	Adj. R^2	RMSE	Variable Entered	Parameter Estimate
Combined	0.518	0.509	0.933	Intercept	-1.27 ± 0.54
				Temperature	0.25 ± 0.023
				Pressure	0.2 ± 0.044
				Humidity x Time constant	-0.16 ± 0.069
				Temperature x Pressure	-0.0087 ± 0.002
SE	0.73	0.725	0.788	Intercept	-3.45 ± 0.44
				Temperature	0.35 ± 0.023
				Pressure	0.2 ± 0.0034
				Temperature x Pressure	-0.0094 ± 0.0018
SH	0.189	0.145	0.964	Intercept	3.79 ± 0.33
				Temperature x Pressure	-0.0045 ± 0.002
				Time constant x ΔC	0.019 ± 0.007
F26	0.218	0.183	0.251	Intercept	6.78 ± 1.24
				Temperature x Humidity	-0.0025 ± 0.0001

There were no differences in variables entered before or after the transformation when increasing the significance level from 0.05 to 0.1. The operation was also repeated by date in addition to by site but failed to significantly improve the model fit.

4.2.2 Discussion

The objective of the experiment was the creation of a model to relate the RSCA data to the flux obtained from the classic chambers. This largely failed as the main factor, CO_2 concentration from the RSCA, was never entered and the models relied largely on temperature as can be seen in Figure 4.6 and 4.8. This created a weak correlation ($R^2 < 0.6$) with the flux from the classic chambers (Figure 4.7). The model however showed high predictions for locations with high actual fluxes. The issues of overestimating the predicted flux in the locations with low actual fluxes may be due to the RSCA extracting soil air from deeper layers or from clogged pores which may be inaccessible to the passive air movement of the classic chambers. The transformation using the natural log of the flux improved the model fit slightly as is expected in the presence of heteroscedasticity, but it still remained relatively low. The best fit of an individual site was for the SE site after the transformation with an adjusted R^2 of 0.73 (using adjusted as multiple variables were entered in the model). This may be due to the SE field having closer to ideal soil conditions, such as medium compaction and humidity, compared to the two other sites. This allowing for cleaner and more homogenous data gathering for the RSCA. While the device's working principle is theoretically the same for all conditions, the effect of less aerated systems

may be amplified in such an active system as opposed to passive soil respiration. The general lack of fit in the models however could potentially stem from the flux data itself as the classic chambers were found to give overly fluctuating data between spatially near replications. Additionally, due to constrains in the sampling procedures of the steady state chambers, the RSCA trials were not taken in the exact same location but within a 50 cm radius from the bases, usually twice on either side of each chamber. This distance may have come to play a role as soil, especially within crop rows, is spatially variable and, due to the chamber area, even micro variations in the terrain can cause significant differences in soil respiration. As the sensor testing revealed, the K30 itself is accurate in stable conditions. A change in concentration is also clearly detected after the pump is activated. This, in conjunction with a drop in pressure inside the headspace of the chamber, indicates that the device is functioning as intended. The issue is therefore in processing the data to a useful form.

While taken close to the point, the RSCA data suffered from variations in soil properties, both due to the natural variations of the soil (texture, micro-topography, etc.) and vegetation (crops and weed causing variations in local CO_2 emissions), but due also to human interference. As the static chambers were fitted on top of a collar installed at the beginning of the season and remaining in the field until the harvest, samplers were careful not to step within the sampling area. This had two effects, the first being that vegetation grew more inside the base than outside, biasing the respiration, and two: the soil directly outside the chamber, where the RSCA was being tested, became unnaturally compacted due to the traffic of the samplers. This is

thought to have had a potentially major impact on the RSCA measurements as a less aerated soil will much less readily let gas escape, especially under the four second suction performed by the device. These high levels of soil variation along with the sensor issues, namely, the time constant of the CO_2 Engine K30 Sensor used on the RSCA being too high to properly capture the actual concentration increase inside the headspace, spurred the need for a more controlled experiment (see section 3.4 Controlled Experiment). The aim was to expose the RSCA to extreme differences in isolated soil properties and observe the effect on the sensor data.

Since the working principle of both types of chambers were radically different, it created difficulties, mainly in modeling the RSCA output to obtain similar flux figures as the static chambers. This was unaided by the classic chambers themselves having shown relatively high, small separation distance variability, in these field conditions. As was shown by Mat-Su (2016), replicate chambers on the same point had as high variability between them as with chambers across a highly variable field in terms of soil properties. Additionally, the sampling of the RSCA could not be performed on the exact soil area as the closed static chambers due to the chamber covers. Waiting until the end of the static chambers trials would only have shifted the time at which the measurements could be taken by more than an hour, changing the ambient conditions, including temperature, which has a sizable impact on soil respiration.

The need for performing the non-linear regression originated from the high and varying time constant as well as some RSCA trials never reaching steady state. These

issues creating difficulties in producing well defined variables. The success of this step allowed for the creation of exact parameters for variable identification. These could be applied to any trial data with ease as their shape was standardized as a first order response. The non-linear regression estimation of the first order response equation constants is however not as reliable as letting the data stabilize naturally. It can potentially find curves in erroneous trials or by estimating plateaus earlier or later than they would naturally be reached. As such, for future field trials and depending on soil composition (higher %O.M), it is suggested to extend the trial times to 5 min instead of 3 min. Other considerations for future field experiments would require higher rigor of foot traffic around the tested area as the chamber is sensitive to even slight soil compaction differences.

4.3 Controlled Experiment

4.3.1 Results

The controlled experiment aim was to induce significant differences in RSCA data by subjecting the soil to extreme treatments. These low and high extremes were created in terms of both humidity and compaction in the first part of the experiment (Figure 4.10 and 4.11) and later by the addition of glucose to the samples (Figure 4.12). These results can be seen by looking at both the pressure and the concentration values of the RSCA. They can be seen in Figures 4.10 and 4.11, respectively. Both pressure and concertation increase as well as their interaction were significant at $p<0.0001$.

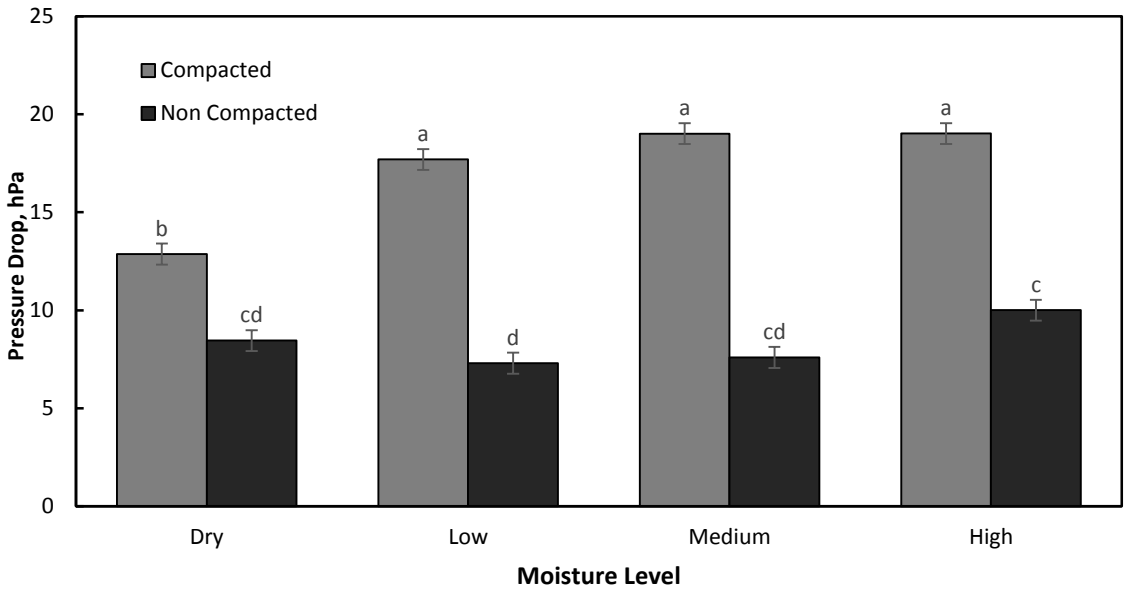

Figure 4.10: Mean pressure drop for the four moisture levels for each of the two compaction levels. Bar height indicates the mean and error bars are +/- 1 standard error. Means sharing the same letter do not differ significantly at the 95% confidence level based on the Tukey mean comparison method

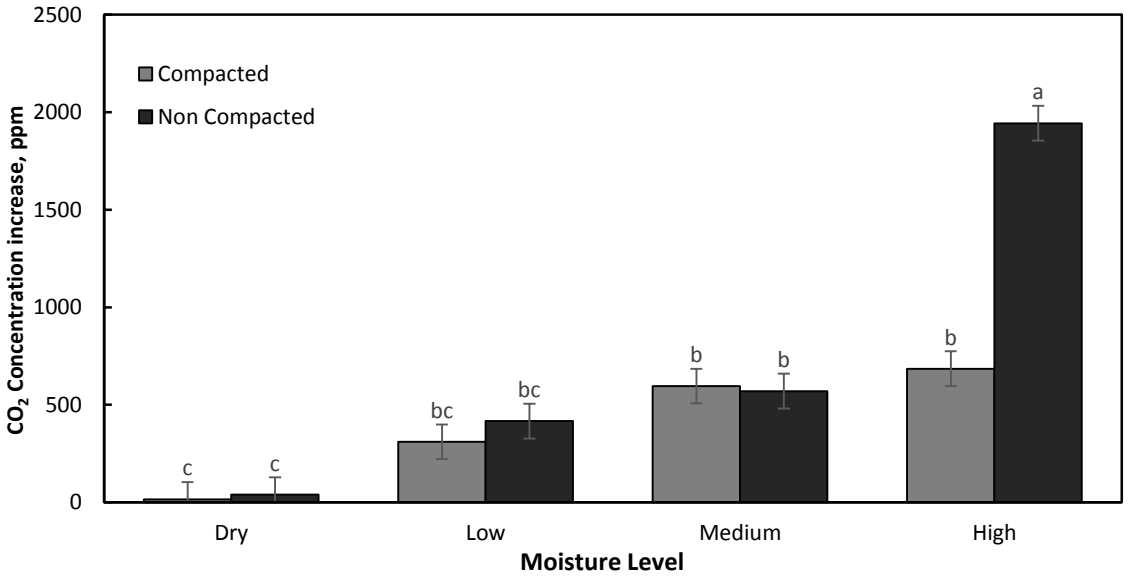

Figure 4.11: Mean CO_2 concentration increase for the four moisture levels for each of the two compaction levels. Bar height indicates the mean and error bars are +/- 1 standard error. Means sharing the same letter do not differ significantly at the 95% confidence level based on the Tukey mean comparison method

Results from the glucose part of the experiment can be seen in Figure 4.12 below. Using the three-way ANOVA, all individual factors as well as the moisture x compaction and moisture x glucose interactions were found to be significant at $p<0.05$. The compaction x glucose interaction and the three-way interactions of moisture x compaction x glucose were not found to be significant ($p>0.05$).

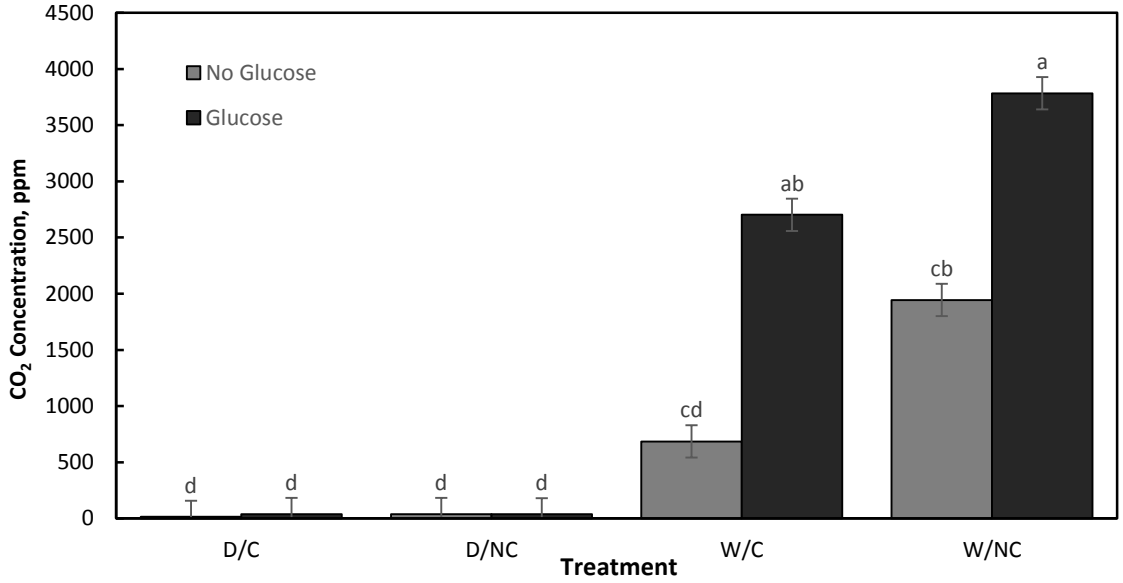

Figure 4.12: Mean CO_2 concentration increase for the wet and dry treatments at both compactions levels and with or without added glucose. Bar height indicates the mean and error bars are +/- 1 standard error. Means sharing the same letter do not differ significantly at the 95% confidence level based on the Tukey mean comparison method

4.3.2 Discussion

The controlled experiment was devised to better understand the factors affecting the measurements obtained by the RSCA. The experiment aims at creating extreme soil respiration inducing environments, both in terms of compaction and humidity, to magnify their effect on the data. The RSCA was additionally modified between the field experiments and the controlled one by the fitting of a fan for air mixing and

preventing high concentration pockets from forming inside the chamber, as well as building in a sampling tube to enable manual sampling of the air inside the headspace.

In contrast to the field experiment, the controlled experiment yielded more conclusive results. As can be seen from Figure 4.10, the soil compaction level had a clear impact on the pressure drop inside the chamber, even in dry soil. The difference between the pressure drops in compacted soils under any of the "low", "medium" or "high" moisture levels was not significantly different. Additionally, in non-compacted soils, slight differences were registered only between the lowest and the highest moisture levels. Figure 4.11 for the CO_2 concentration increase shows a significant difference between the non-compacted, high moisture treatment and the rest of the treatments. Aside from that, the other non-dry moisture levels are not considered significantly different from each other. The "low" moisture level also is shown not to be significantly different in CO_2 concentration increase from the dry soil. Aside from the non-compacted high moisture treatment, there were no differences between compacted and non-compacted soils of the same moisture level.

The substrate induced respiration test results are shown in Figure 4.12; it can be seen that the addition of glucose significantly affected the soil respiration. This was however only true in the wet soils and, in line with the previous results, more pronounced in the non-compacted soils. This result, albeit originating from a controlled lab setting, additionally supports the validity of the RSCA. A steep increase in CO_2 concentration can be expected with the addition of glucose, feeding the micro-

organisms in the soil. These being close to non-existent in the dry soil easily explains their lack of improvement after the glucose addition.

It is still impossible to tell whether the lower concentrations noted in compacted soils can be attributed to a lower CO_2 production due to aeration issues inside the soil or to the pump system being unable to vacuum as much air as in the non-compacted soils. While this is an issue, it is also potentially representative of the natural occurrence of air being trapped in the soil because of high compaction levels, hence, being unable to naturally escape the soil surface. Improvements to this experiment would be a proliferation of factor levels. Intermediate compactions and moisture levels would greatly help in finding the respiration peaks for both factors. Additionally, sending soil for a laboratory respiration test for each of these levels would reveal any disparity, if it existed, between the relative concentration increases at each level by the RSCA and in the lab. Other potential factors may also be tested in a similar experimental setup, such as temperature or varying soils textures. Finally, testing the closed static chambers in parallel to the RSCA in such a controlled environment would be ideal for the attempt at modeling the RSCA data to equate the flux estimates from the classic chambers. The homogeneity of the soils in the controlled trials being of great help for such an endeavor.

Chapter 5 Conclusions

The RSCA was developed as a low-cost, portable instrumentation system for *in situ* assessment of soil respiration. The RSCA, as a device, functions as intended and allows the vacuuming of soil air into the headspace, letting it be measured by the various on-board sensors. The main sensor, the CO_2 Engine K30, was tested during normal operation of the device and found to be accurate in stable conditions. Testing this sensor allowed for a better understanding of the RSCA's limits and capabilities. The software that was created to process the sensor data is both robust and flexible. It organized the data and output representative parameters for the user. The interpretation of two of these factors, pressure drop and concentration increase, over various treatments shows the chamber to be reacting as predicted to changes in the soil. The RSCA is sensitive to varying moisture and compactions levels. This explains the inconclusive results of the field experiment that compared RSCA responses to corresponding CO2 flux measurements. Micro variations in soil topography as well as human disruption of the sampling environment make it difficult to relate the RSCA data to the flux obtained from the classic chambers. While this is an issue, as flux is a standard and acceptable way to relay soil respiration, the controlled experiment has shown promise in relating soil conditions to the RSCA measurement.

Future testing of the device would require a more precise and reliable comparison than the steady state chambers could offer. This project additionally highlighted the capabilities and limitations in the use of NDIR sensors with high time constants in field conditions. While the readings may be correct, the chamber is adversely affected

by small variations in soils conditions; this is actually a detriment to the goal of mapping the field by sampling at representative locations. Knowing this however, and by tailoring the sampling time of the RSCA to the study site, the device is capable of taking a multitude of points in a relatively short time. This hopefully allows for some averaging and interpolation across zones, giving a more complete idea of the field's soil respiration's spatial heterogeneity than by using very limited numbers of static chamber locations. Using the different sensors, the RSCA could ideally detect zones of compaction or high microbial activity. Coupled with the on-board GPS, this would provide an additional layer of understanding in precision agriculture, upon which to base prescription maps, or to better predict yields.

The field experiment of this study compared the RSCA to the closed static chambers as they constitute an accepted method of quantifying soil respiration. These were highly variable even between replicates, as well as time and labor intensive. This without being cheaper because of the number needed. Other measurement methods and chamber styles exist (often also using a non-dispersive infrared spectroscopy measurement principle), such as open chambers and eddy covariance towers, these are however expensive and are of a much higher complexity to construct. The RSCA's total component price does not exceed $500 CAD. Additionally, all components are readily purchasable in parts and the construction process is not overly complex. As such, provided further development, the RSCA could provide a low-budget, yet reliable alternative to currently existing methods. Its automation aspect along with its georeferencing also make it a prime candidate for on-the-go implementation.

Soil respiration sensing as it pertains to agricultural fields is currently mostly an academic endeavour, used mainly for research in environmental studies. The potential of such measurements for agricultural production is found in its relation to microbial activity, indicating the general health of the soil. If, in addition to this, devices such as the RSCA are used, which are more complete with full sensor batteries, the understanding of micro and macro variations in soil properties across a field might help in the crop production aspect. As far as the technology itself however, the future of gas sensing lies in long term readings and trends. Readings over short periods of time will show too much variation to make a proper assessment of the site, differences in soil respirations are to be measured in terms of years or at least months. Obtaining such trends for specific sites and understanding their cause may result in new, potentially untapped, sources of georeferenced information.

List of References

Atkin Owen, K.O., Tjoelker, M.G. 2003. Thermal acclimation and the dynamic response of plant respiration to temperature. *Trends in Plant Science*, **8**(7), 343-51.

Berg, B., Staaf, H., Wessen, B. 1987. Decomposition and Nutrient Release in Needle Litter from Nitrogen-fertilized Scots Pine (Pinus sylvestris) Stands. *Scandinavian Journal of Forest Research*, **2**(1-4), 399-415.

Burton, A.J., Pregitzer, K.S., Zogg, G.P., Zak, D.R. 1996. Latitudinal variation in sugar maple fine root respiration. *Canadian Journal of Forest Research-Revue Canadienne De Recherche Forestiere*, **26**(10), 1761-1768.

Craine, J.M., Wedin, D.A., Chapin, F.S. 1999. Predominance of ecophysiological controls on soil CO2 flux in a Minnesota grassland. *Plant and Soil*, **207**(1), 77-86.

Crawford, R.M.M. 1992. Oxygen Availability As An Ecological Limit To Plant-Distribution. *Advances in Ecological Research*, **23**, 93-185.

Currie, J.A. 1974. Soil respiration. *Min. Agric., Fish, Food, Tech*, **29**, 459-466.

Davidson, E.A., Janssens, I.A., Luo, Y. 2006. On the variability of respiration in terrestrial ecosystems: moving beyond Q10. *Global Change Biology*, **12**(2), 154-164.

Davidson, E.A., Savage, K., Verchot, L.V., Navarro, R. 2002. Minimizing artifacts and biases in chamber-based measurments of soil respiration. *Agricultural and Forest Meteorology*, **113**, 21-37.

Davidson, E.A., Verchot, L.V., Cattanio, J.H., Ackerman, I.L., Carvalho, J.E.M. 2000. Effects of soil water content on soil respiration in forests and cattle pastures of eastern Amazonia. *Biogeochemistry*, **48**(1), 53-69.

De Vries, F.W.T.P. 1975. The Cost of Maintenance Processes in Plant Cells. *Annals of Botany*, **39**(1), 77-92.

Dörr, H., Münnich, K.O. 2011. Annual variation in soil respiration in selected areas of the temperate zone. *Tellus B; Vol 39, No 1-2 (1987)*.

Eshel, G., Lifschitz, D., Bonfil, D.J., Sternberg, M. 2014. Carbon exchange in rainfed wheat fields: Effects of long-term tillage and fertilization under arid conditions. *Agriculture Ecosystems & Environment*, **195**, 112-119.

Fang, C., Moncrieff, J.B. 2000. The dependence of soil CO2 efflux on temperature. *Soil Biology and Biochemistry*, **33**, 155-165.

Fernandez, G.C.J. 1992. Residual Analysis And Data Transformations - Important Tools In Statistical-Analysis. *Hortscience*, **27**(4), 297-300.

Fogel, R., Cromack, K. 1977. Effect Of Habitat And Substrate Quality On Douglas-Fir Litter Decomposition In Western Oregon. *Canadian Journal of Botany*, **55**(12), 1632-1640.

Government of Canada. 2013. Agricultural Greenhouse Gases Program, Vol. 2016.

Han, H.F., Ning, T.Y., Li, Z.J., Cao, H.M. 2014. Soil respiration rate in summer maize field under different soil tillage and straw application. *Maydica*, **59**(1-4), 187-196.

Hanson, P.J., Edwards, N.T., Garten, C.T., Andrews, J.A. 2000. Separating root and soil microbial contributions to soil respiration: A review of methods and observations. *Biogeochemistry*, **48**(1), 115-146.

Healy, R.W., Striegl, R.G., Russell, T.F., Hutchinson, G.L., Livingston, G.P. 1995. Numerical Evaluation of Static-Chamber Measurements of Soil—Atmosphere Gas Exchange: Identification of Physical Processes. *Soil Science*, **50**(3), 740-747.

Hillel, D. 1998. *Environmental Soil Physics*. Press/Elsevier, San Diego, CA.

Hoff, J.H.v.t. 1884. *Etudes de dynamique chimique*. Frederik Muller, Amsterdam.

Hogberg, P., Nordgren, A., Buchmann, N., Taylor, A.F.S., Ekblad, A., Hogberg, M.N., Nyberg, G., Ottosson-Lofvenius, M., Read, D.J. 2001. Large-scale forest girdling shows that current photosynthesis drives soil respiration. *Nature*, **411**(6839), 789-792.

Holland, E.A., Robertson, G.P., Greenberg, J., Groffman, P., Boone, R., Gosz, J. 1999. *Soil CO2, N2O, and CH4 Exchange*. Oxford University Press, New York, New York, USA.

Hutchinson, G.L., Livingston, G.P. 2001. Vents and seals in non-steady-state chambers used for measuring gas exchange between soil and the atmosphere. *Soil Science*, **52**, 675-682.

Jabro, J.D., Sainju, U., Stevens, W.B., Evans, R.G. 2008. Carbon dioxide flux as affected by tillage and irrigation in soil converted from perennial forages to annual crops. *Journal of Environmental Management*, **88**(4), 1478-1484.

Kaur, J., Adamchuk, V.I., Whalen, J.K., Ismail, A.A. 2015. Development of an NDIR CO(2) sensor-based system for assessing soil toxicity using substrate-induced respiration. *Sensors (Basel)*, **15**(3), 4734-48.

Kowalenko, C.G., Ivarson, K.C., Cameron, D.R. 1978. Effect Of Moisture-Content, Temperature And Nitrogen-Fertilization On Carbon-Dioxide Evolution From Field Soils. *Soil Biology & Biochemistry*, **10**(5), 417-423.

Lambers, H., Steingrover, E. 1978. Efficiency Of Root Respiration Of A Flood-Tolerant And A Flood-Intolerant Senecio Species As Affected By Low Oxygen-Tension. *Physiologia Plantarum*, **42**(2), 179-184.

Lewicki, J.L., Evans, W.C., Hilley, G.E., Sorey, M.L., Rogie, J.D., Brantley, S.L. 2003. Shallow soil CO2 flow along the San Andreas and Calaveras Faults, California. *Journal of Geophysical Research-Solid Earth*, **108**(B4), 14.

Linn, D.M., Doran, J.W. 1984. Effect Of Water-Filled Pore-Space On Carbon-Dioxide And Nitrous-Oxide Production In Tilled And Nontilled Soils. *Soil Science Society of America Journal*, **48**(6), 1267-1272.

Liu, X.Z., Wan, S.Q., Su, B., Hui, D.F., Luo, Y.Q. 2002. Response of soil CO2 efflux to water manipulation in a tallgrass prairie ecosystem. *Plant and Soil*, **240**(2), 213-223.

Livingston, G.P., Hutchinson, G.L., Spartalian, K. 2005. Diffusion theory improves chamber-based measurements of trace gas emissions. *Geophysical Research Letters*, **32**(24).

Lundergardh, H. 1922. Neue Apparate zur Analyse des Kohlensauregehalts der Luft. *Biochem Z*.

Luo, Y., Zhou, X. 2006. Chapter 3 - Processes of CO2 Production in Soil. in: *Soil Respiration and the Environment*, Academic Press. Burlington, pp. 35-59.

Martin, J.G., Bolstad, P.V. 2005. Annual soil respiration in broadleaf forests of northern Wisconsin: influence of moisture and site biological, chemical, and physical characteristics. *Biogeochemistry*, **73**(1), 149-182.

Mat-Su, A. 2016. Application of Proximal Soil Sensing For Environmental Characterization of Agricultural Land. in: *Bioresource Engineering*, Vol. MS Thesis, McGill University. Montreal, Quebec, pp. 130.

McInerney, M., Bolger, T. 2000. Temperature, wetting cycles and soil texture effects on carbon and nitrogen dynamics in stabilized earthworm casts. *Soil Biology & Biochemistry*, **32**(3), 335-349.

Nay, S.M., Mattson, K.G., Bormann, B.T. 1994. Biases of Chamber methods for Measuring Soild CO2 Efflux Demonstrated with a Laboratory Aparatus. *Ecology*, **75**(8), 2460-2463.

Papendick, R.I., Camprell, G.S. 1981. Theory and Measurement of Water Potential1. in: *Water Potential Relations in Soil Microbiology*, Soil Science Society of America. Madison, WI.

Pavia, D.L., Lampman, G.M., Kriz, G.S. 1988. *Introduction to Laboratory Techniques: A Contemporary Approach*. *3rd ed*. Saunders College Pub, Philadelphia.

Porkka, O.H. 1931. Uber eine neue Methode zur Bestimmung der Bodenatmung. *Ann Soc Zool-Bot Fenn Yanamo*.

Pumpanen, J., Kolari, P., Ilvesniemi, H., Minkkinen, K., Vesala, T., Niinistö, S., Lohila, A., Larmola, T., Morero, M., Pihlatie, M., Janssens, I., Yuste, J.C., Grünzweig, J.M., Reth, S., Subke, J.-A., Savage, K., Kutsch, W., Østreng, G., Ziegler, W., Anthoni, P., Lindroth, A., Hari, P. 2004. Comparison of different chamber techniques for measuring soil CO2 efflux. *Agricultural and Forest Meteorology*, **123**(3-4), 159-176.

Pumpanen, J., Longdoz, B., Kutsch, W.L. 2009. Field measurments of soil respiration: principles and constraints, potentials and limitations of different methods. in: *Soil Carbon Dynamics: An integrated Methodology*, (Eds.) W.L. Kutsch, M. Bahn, A. Heinemeyer, Cambridge University Press. New York, USA.

Raich, J.W., Tufekcioglu, A. 2000. Vegetation and soil respiration correlations and controls. *Biogeochemistry*, **40**, 71-90.

Rice, C.W., Smith, M.S. 1982. Denitrification in no-till and Plowed Soils. *Soil Science Society of America Journal*, **46**(6), 1168-1173.

Richards, B.N. 1987. *The microbiology of terrestrial ecosystems*. John Wiley and Sons Inc., New York, NY, USA.

Rochette, P., Desjardins, R.L., Pattey, E. 1991. Spatial and Temporal Variability of Soil Respiration in Agricultural Fields. *Canadian Journal of Soil Science*, **71**(2), 189-196.

Rochette, P., Hutchinson, G.L. 2005. Measurement of soil respiration in situ: chamber techniques.

Rolston, D.E. 1986. Gas Diffusivity. in: *Methods of Soil Analysis: Part 1—Physical and Mineralogical Methods*, Soil Science Society of America, American Society of Agronomy. Madison, WI.

Ruser, R., Flessa, H., Russow, R., Schmidt, G., Buegger, F., Munch, J.C. 2006. Emission of N2O, N2 and CO2 from soil fertilized with nitrate: effect of compaction, soil moisture and rewetting. *Soil Biology and Biochemistry*, **38**(2), 263-274.

Schlentner, R.E., Cleve, K.V. 1985. Relationships between CO2 evolution from soil, substrate temperature, and substrate moisture in four mature forest types in interior Alaska. *Forest Research*, **15**(1), 97-106.

SenseAir. 2012. Pressure Dependence of SenseAir's NDIR sensors, Data Sheet.

Singh, J., Gupta, S. 1977. Plant Decomposition and Soil Respiration in Terrestrial Ecosystems. *Botanical Review*, **43**(4), 449-528.

Skoog, D.A., Holler, F.J., Nieman, T.A. 1998. *Principles of instrumental analysis*. Saunders College Pub. ; Harcourt Brace College Publishers, Philadelphia; Orlando, Fla.

Smith, K.A., Ball, T., Conen, F., Dobbie, K.E., Massheder, J., Rey, A. 2003. Exchange of greenhouse gases between soil and atmosphere: interactions of soil physical factors and biological processes. *Soil Science*, **54**, 779-791.

Smith, P., Martino, D., Cai, Z., Gwary, D., Janzen, H., Kumar, P., McCarl, B., Ogle, S., O'Mara, F., Rice, C., Scholes, B., Sirotenko, O. 2007. Agriculture. in: *In Climate Change 2007: Mitigation. Contribution of Working Group III to the Fourth Assessment Report of the Intergovernmental Panel on Climate Change*, (Eds.) B. Metz, O.R. Davidson, P.R. Bosch, R. Dave, L.A. Meyer, Cambridge University Press. Cambridge, United Kingdom and New York, NY, USA.

Stotzky, G., Norman, A.G. 1961. Factors limiting microbial activities in soil. *Archiv für Mikrobiologie*, **40**(4), 341-369.

Sun, Y.W., Liu, W.Q., Zeng, Y., Wang, S.M., Huang, S.H., Xie, P.H., Xiao-Man, Y. 2011. Water Vapor Interference Correction in a Non Dispersive Infrared Multi-Gas Analyzer. *Chinese Physics Letters*, **28**(7), 4.

Vance, E.D., Chapin, F.S. 2001. Substrate limitations to microbial activity in taiga forest floors. *Soil Biology and Biochemistry*, **33**(2), 173-188.

Wang, Amudson, R., Trumbore, S. 1999. The impact of land use change on C turnover in soils. *Global Biogeochemical Cycles*, **13**(1), 47-57.

Wang, Nakayama, M., Yagi, M., Nishikawa, M., Fukunaga, M., Watanabe, K. 2005. The NDIR CO2 monitor with smart interface for global networking. *Ieee Transactions on Instrumentation and Measurement*, **54**(4), 1634-1639.

Wildung, R.E., Garland, T.R., Buschbom, R.L. 1975. The interdependent effects of soil temperature and water content on soil respiration rate and plant root decomposition in arid grassland soils. *Soil Biology and Biochemistry*, **7**(6), 373-378.

Witkamp, M. 1966. Rates of Carbon Dioxide Evolution from Forest Floor. *Ecology*, **47**(3), 492.

Xu, M., Qi, Y. 2001. Spatial and seasonal variations of Q(10) determined by soil respiration measurements at a Sierra Nevadan forest. *Global Biogeochemical Cycles*, **15**(3), 687-696.

Yasuda, T., Yonemura, S., Tani, A. 2012. Comparison of the Characteristics of Small Commercial NDIR CO2 Sensor Models and Development of a Portable CO2 Measurement Device. *Sensors*, **12**(3), 3641-3655.

Appendices

Appendix A: Technical Drawings (not to scale, all dimensions in mm)

A1- Drawing and important dimensions of main PVC cylinder for the RSCA

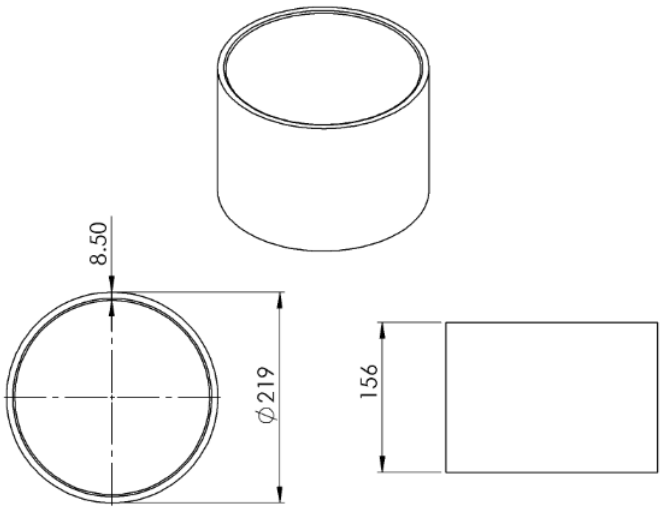

A2- Drawing and important dimensions of metal cutting disk for the RSCA

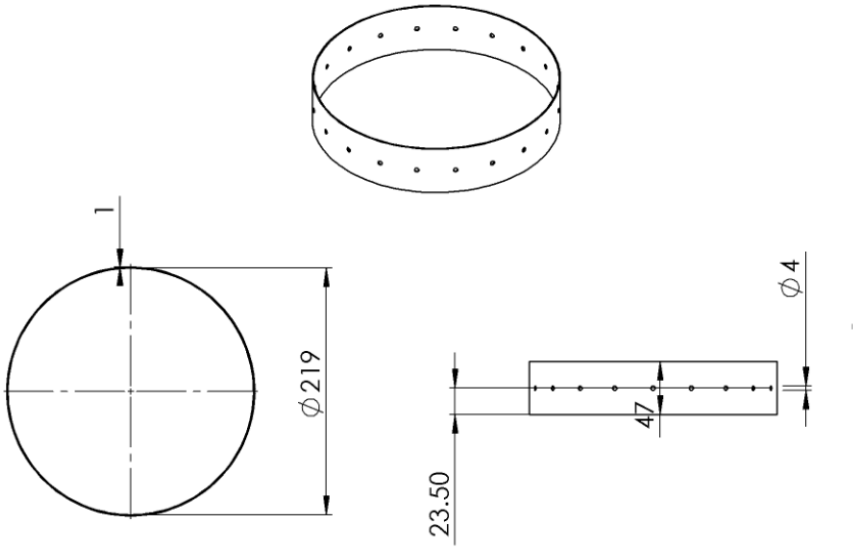

A3- Drawing and important dimensions of main delrin plate

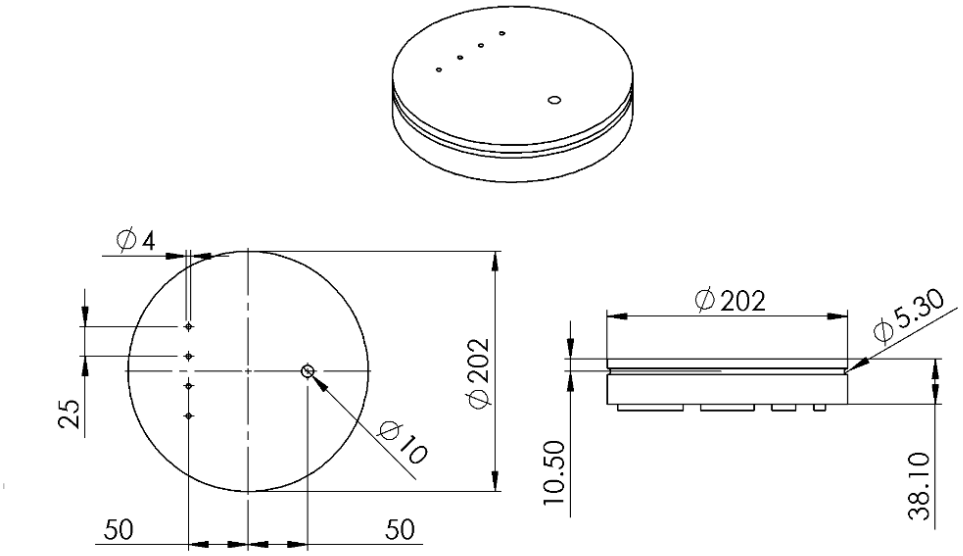

A4- Drawing and important dimensions of delrin ECU slab

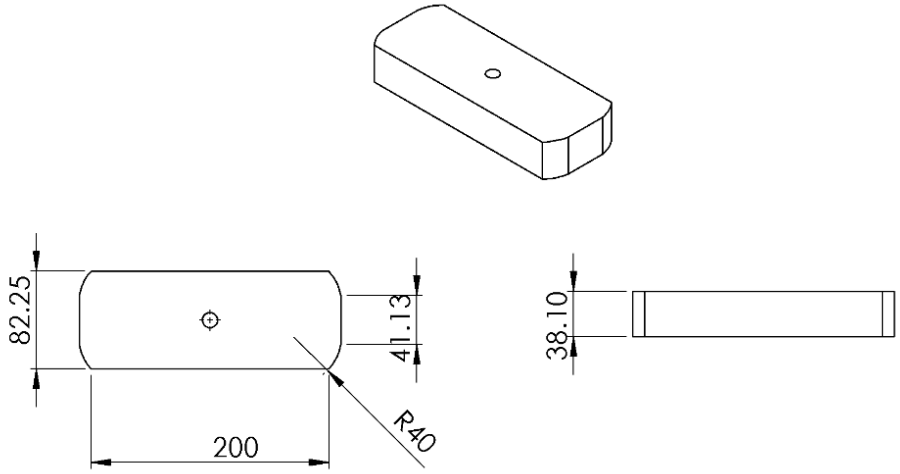

A5- Drawing and important dimensions of 3D printed relay protector

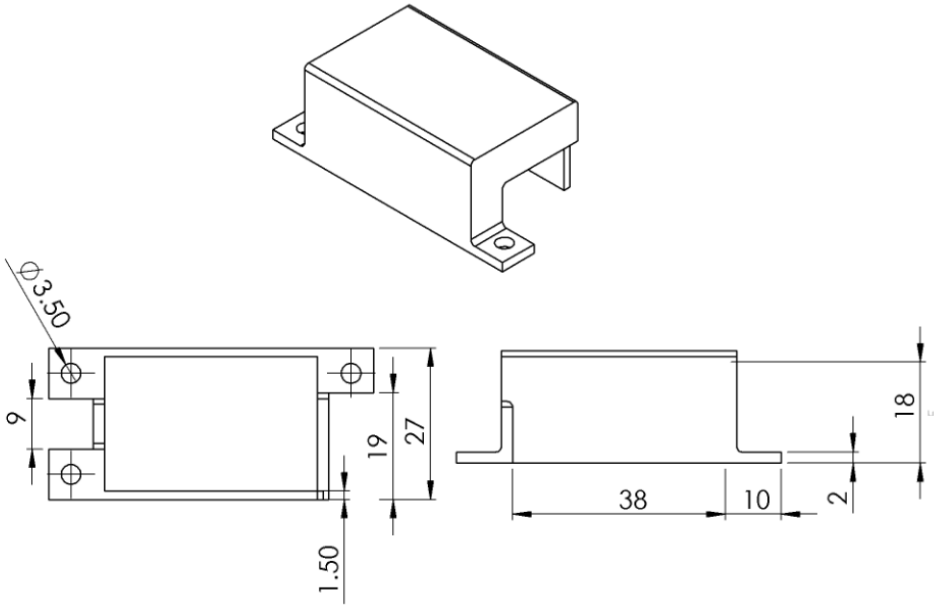

A6- Drawing and important dimensions of 3D printed battery holder

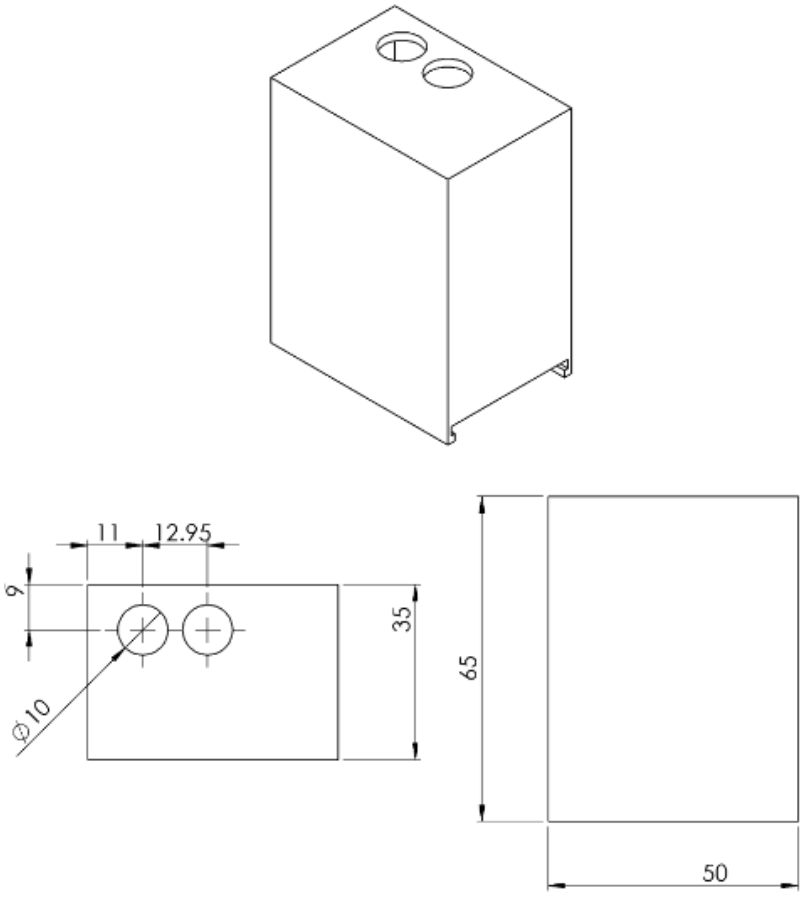

A7- Drawing and important dimensions of 3D printed battery holder (cover)

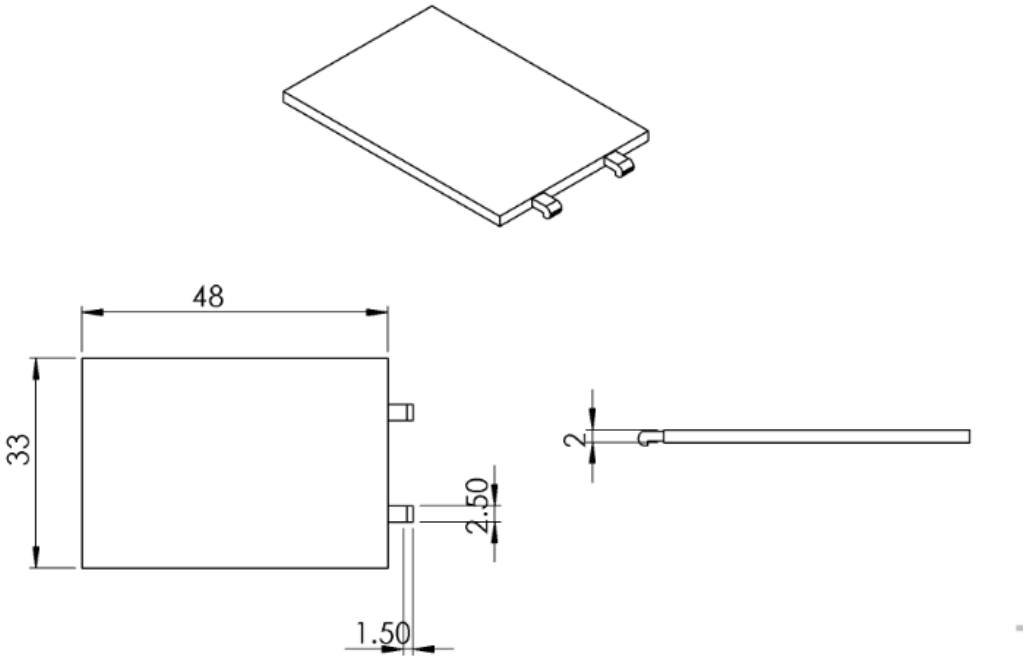

A8- 3D render of first RSCA prototype

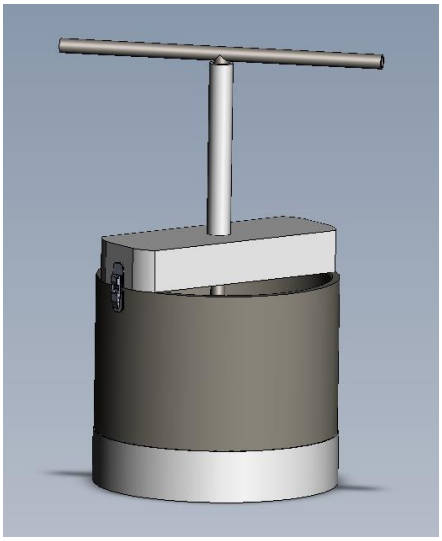

Appendix B: MATALB®, Python™, Arduino and SAS code

B1- RSCA Arduino code

```
/*
 Last update 22/07/2015
 by Florian Reumont

 RSCA Main Control Code
 */

// INCLUDE LIBRARIES
#include <SD.h>                      // Add SD card Library
#include "DHT.h"                    // Add RH sensor Library
#include "Adafruit_GPS.h"           //Add GPS Shield Library
#include <SoftwareSerial.h>
#include <Wire.h>
#include <Adafruit_Sensor.h>      //Add Libraries for BMP180 sensor
#include <Adafruit_BMP085_U.h>

//  ASSIGN PINS
#define KseriesTX 2      // Transmit pin for the K30 CO2 sensor
#define KseriesRX 3      // Receive pin for the K30 CO2 sensor
#define DHTPIN 4        // Assign Pin for RH sensor
#define Relay 5         // Relay Signal Pin
#define GpsRX 7         //RX (receive pin) of GPS shield
#define GpsTX 8         //TX (transmit pin) of GPS shield
#define SDPin 10        // Assign Pin for SD card shield, should not be
used on sensor shield
#define ButtonPin 14    // Assign Analog Pin for button
#define LedPin 15        // Assign Pin for LED
#define echoPin 17       // Assign Echo Pin for the Ultrasound
#define trigPin 16       // Assign Trig pin for the Ultrasound
#define DHTTYPE DHT11   // DHT 11 type sensor
//#define FanPin 9
DHT dht(DHTPIN, DHTTYPE);

//  DEFINE SERIAL COMUNICATION PINS
SoftwareSerial GpsSerial(GpsTX, GpsRX);
//Initialize Ultimate GPS sensor shield with pin 7 as Rx and 8 as Tx
SoftwareSerial K_30(KseriesTX,KseriesRX);
//Initialize kSeries Sensor with pin 2 as Rx and 3 as Tx
Adafruit_BMP085_Unified bmp = Adafruit_BMP085_Unified(10085);       //
Initialize BMP180 Pressure sensor

// DEFINE VARIABLES
byte readCO2[] = {0xFE, 0X44, 0X00, 0X08, 0X02, 0X9F, 0X25};
//Command packet to read Co2 (see app note)
byte response[] = ;                                    //create an array
to store the response
#define PMTK_SET_NMEA_UPDATE_1HZ  "$PMTK220,1000*1F"                   //
Set GPS to update at 1Hz
#define PMTK_SET_NMEA_OUTPUT_GGAONLY
"$PMTK314,0,0,0,1,0,0,0,0,0,0,0,0,0,0,0,0,0,0*29"   // Only request
the GGPA line from GPS communication
```

```
#define PMTK_Q_RELEASE "$PMTK605*31"
String CharString = "";                                          // a
string to hold incoming data
const unsigned int baud = 9600;                                  //
Bits per second
double duration, distance;                                        //
Long variables for the Ultrasound sensor
unsigned long Time = 301000;
// Set time higher than breakoff limit for logging
unsigned long valCO2;
File myFile;
unsigned long Delay;
unsigned long TimeElapsed;


// -----------------VOID SETUP-----------------------
void setup() {

  Serial.begin(baud);       //Begin Hardware Serial communication, only
needed if printing to serial
  GpsSerial.begin(baud);   // Begin Software Serial Comunication for GPS
chip
  K_30.begin(baud);        //Begin Software Serial Communication for K30
CO2 sensor
  dht.begin(); // Start the DHT sensor Library

  delay(2000);

  pinMode(trigPin, OUTPUT);
  pinMode(echoPin, INPUT);
  pinMode(SDPin, OUTPUT);
  pinMode(ButtonPin, INPUT_PULLUP);
  pinMode(LedPin, OUTPUT);
  pinMode(Relay, OUTPUT);
//  pinMode(FanPin, OUTPUT);

  if(!bmp.begin()){
//    Serial.print("BMP180 initialization failed!");
  } else{
    Serial.println("BMP180 Working");
  }
  if (!SD.begin(SDPin)) {                          //Checking if SD card
was properly found and is ready to be written onto
//    Serial.println("SD initialization failed!");
  } else{
    Serial.println("SD Working");
  }

  GpsSerial.println(PMTK_Q_RELEASE);
  GpsSerial.println(PMTK_SET_NMEA_OUTPUT_GGAONLY);
  GpsSerial.println(PMTK_SET_NMEA_UPDATE_1HZ);
  CharString.reserve(80);               //Reserve space for the upcoming
GPS characters

}

// -----------------VOID LOOP---------------
```

```
void loop() {

  unsigned long time1 = millis();    //Log the starting time of the loop

  digitalWrite(LedPin, LOW);       // Turn LED off

    // Button Check                //Only check the button value if the
timer isn't already running, this prevents the clock from re-setting
halfway through sampling
  if(Time > 149000) {
//    digitalWrite(FanPin, LOW);
    int ButtonValue = digitalRead(ButtonPin);
    if(ButtonValue == LOW) {            // Button pin is pulled up,
hence when the button is pressed the pin will read as low as it is now
connected to ground
      Time = 0;
    }
  }
//else{
//    digitalWrite(FanPin, HIGH);
//  }

  delay(10);

  // CO2 SENSOR READING
  K_30.listen();                //Switch the Software Serial to
listening to the K30
  if(K_30.isListening()){
    sendRequest(readCO2);
    valCO2 = getValue(response);
    Serial.println(valCO2);
    Serial.println("K_30 is Listening");
  }

  delay(10);

  //PRESSURE SENSOR READING
  sensors_event_t event;
  bmp.getEvent(&event);

//  delay(10);
//
//  // ULTRASOUND SENSOR READING
//  digitalWrite(trigPin, LOW);
//  delayMicroseconds(2);
//  digitalWrite(trigPin, HIGH);
//  delayMicroseconds(10);
//  digitalWrite(trigPin, LOW);
//  duration = pulseIn(echoPin, HIGH);
//  distance = ((duration/2) / 29.1)+1.5;       // the +1.5 takes into
account the height of the sensor

  delay (10);

  // RH SENSOR READING
  float temperature = dht.readTemperature();  // Reading temperature or
humidity takes about 250 milliseconds!
```

```
  float humidity = dht.readHumidity();     // Sensor readings may also
be up to 2 seconds 'old' (its a very slow sensor)

  delay (10);

  // GPS SENSOR READING
  if(Time <= 12000){            //Only read the GPS data for the first 4
data points
    GpsSerial.listen();      //Switch to listening to the GPS Shield
    if (GpsSerial.isListening()){
//    Serial.println("GPS is Listening");
      while (true) {
        char c = GpsSerial.read();
        if(c != (char)-1 ){
          CharString += c;
        }
        if (c == '\n'){
          break;
        }
      }
    }
  }

  //WRITE TO FILE
  if( Time < 150000) {         //If within the sampling period, write to
the SD card
    digitalWrite(LedPin, HIGH);
    myFile = SD.open("GAS.txt", FILE_WRITE);  // Open OR Create the file
with chosen name and choose weather to write or read it (write in this
case)
//    Serial.print("myFile Status:  ");
//    Serial.println(myFile);
    if (myFile) {
//      Serial.print("Writing to test.txt...");
      myFile.print(Time);
      myFile.print(",");
//      myFile.print(distance);
//      myFile.print(",");
      myFile.print(valCO2);
      myFile.print(",");
      myFile.print(temperature);
      myFile.print(",");
      myFile.print(event.pressure);
      myFile.print(",");
      myFile.print(humidity);
      myFile.print(",");
      if(Time <= 12000){            //Only write GPS data on the first 4
data points
        myFile.print(CharString);
      }else{
        myFile.println("");
      }
      // close the file:
      myFile.close();      //close the file;
    } else {
      for (int b = 0; b <= 3; ++b){     //Warning light if SD Card is
missing or malfunctioning
```

```
        digitalWrite(LedPin, LOW);
        delay(400);
        digitalWrite(LedPin, HIGH);
        delay(400);
        Serial.println(b);
      }
      Serial.println("error opening test.txt");  // if the file didn't
open/*
    }
  }

  CharString = "";   // Clear Charstring GPS
  unsigned long time2 = millis();    // log time at the end of the loop
  Time = Time+ (time2-time1);       // calculate how long the loop took
to run

  if (Time >= 20000 && Time <= 24000){
    digitalWrite(Relay, HIGH);
    }
    else {
      digitalWrite(Relay, LOW);
      }

  Serial.println(Time);

   //WRITE TO SERIAL (OPTIONAL)          // Comment this back in for
troubleshooting via serial
  Serial.print(Time);
  Serial.print("s , ");
  Serial.print(distance);
  Serial.print("cm , ");
  Serial.print(humidity);
  Serial.print(" % humidity , ");
  Serial.print(temperature);
  Serial.print(" Degree , ");
  Serial.print(valCO2);
  Serial.print("ppm ,  ");
  Serial.print(event.pressure);
  Serial.print("atm, ");
  Serial.print(CharString);
//  Serial.print("Button State: ");
//  Serial.print(digitalRead(ButtonPin));
  Serial.print(", Delay: ");
  Serial.println(Delay);
  Serial.print("File Status:  ");
  Serial.println(myFile);
  Serial.println("");

}


// -----------------FUNCTIONS---------------------------

void sendRequest(byte packet[]){
 while(!K_30.available()){ //keep sending request until we start to get
a response
 K_30.write(readCO2,7);
```

```
 delay(50);
 }

 int timeout=0; //set a timeoute counter
 while(K_30.available() < 7 ){ //Wait to get a 7 byte response
 timeout++;
 if(timeout > 10){ //if it takes to long there was probably an error
 while(K_30.available()) //flush whatever we have
 K_30.read();
 break; //exit and try again
 }
 delay(50);
 }

 for (int i=0; i < 7; i++){
 response[i] = K_30.read();
 }
}

unsigned long getValue(byte packet[])
{
 int high = packet[3]; //high byte for value is 4th byte in packet in
the packet
 int low = packet[4]; //low byte for value is 5th byte in the packet
 unsigned long val = high*256 + low; //Combine high byte and low byte
with this formula to get value
 return val;
}

//end
```

B2- MATLAB® code for RSCA data processing

```
close all; clear ; clc; rehash;
tic
disp('RSCA Filtering');
disp('Author: Florian Reumont, Bioresource Eng. Department, McGill
University');
disp('Email: florian.reumont@mail.mcgill.ca');
disp('  ');
%% Last updated: October 21, 2015

%% GLOBAL INPUT VARIABLES
% INPUT FILES
inName = 'AllDays_Master.xlsx'; % Input filename

%% USER INPUT
site = input('Which study site? (Ans:1=SE/2=SH/3=F26/4=Custom) : ');

disp ' '
% Site, planting and harvest date setting
if site == 1    % SE: St-Emmanuel
    inSheet = 'SE';

elseif site == 2   % SH: Sherington
    inSheet = 'SH';
```

```
elseif site == 3    % F26: Field 26
    inSheet = 'Field26';

elseif site == 4   %Custom number of samples
    inSheet = 'Sheet1';

else
    disp 'Please input correct site name!'
end

%% LOCAL VARIABLES
% Converstion factors of 1ppmv unit to mg/m^3
K30Limit = 10000;  %Upper K30 sensor limit in ppm
DataRange = 'A:F';
StartTrial = 1;

%% Import Excel Data
[data, text, raw] = xlsread(inName, inSheet, DataRange);  %import data

%% Split Input data between trial Runs and Store in a Cell Array

for ii=1:size(data,1);
    if data(ii,2)==0 || ii == size(data,1);
        if ii > 1;
            if ii == size(data,1);
                EndTrial = ii;
            else
                EndTrial = ii-1;
            end
            if exist('TrialArray','var') == 0;
                TrialArray = cell(1,1);
                a = 1;
            else
                a = a+1;
            end
            TrialArray = data(StartTrial:EndTrial,:);
        end
        StartTrial = ii;
    end
end

%% Filter Data and create slope
MaxConcentrationArray = (zeros(size(TrialArray,2),1)*NaN);
MinConcentrationArray = MaxConcentrationArray;
MaxHumidityArray = MaxConcentrationArray;
MinHumidityArray = MaxConcentrationArray;
MeanTemperatureArray = MaxConcentrationArray;
MinPressureArray = MaxConcentrationArray;
DiffPressureArray = MaxConcentrationArray;
TimeShift = MaxConcentrationArray;
ConcShift = MaxConcentrationArray;
FinalTrialArray = cell(size(TrialArray));


for ii = 1: size(TrialArray,2);
    PressureCorrection = zeros(size(TrialArray,1),1)*NaN;
```

```
    Concentration = zeros(size(TrialArray,1),1)*NaN; %Empty array not to
overwrite original

    for jj = 1 : size(Concentration,1);
        PressureCorrection(jj) = (TrialArray(jj,3))/(((4.026*10^-
3)*(TrialArray(jj,5)/10))+((5.78*10^-5)*(TrialArray(jj,5)/10)^2));
        if (TrialArray(jj,3)>= K30Limit)|| PressureCorrection(jj)< 300;
            PressureCorrection(jj) = NaN;
            Concentration(jj) = NaN;
            TrialArray(jj,3) = NaN;
        else
            Concentration(jj) = (PressureCorrection(jj)* 12.0107 * 1)/ (
0.0821 * (TrialArray(jj,4)+273.15)) ;
        end
        TrialArray(jj,2) = (TrialArray(jj,2))/1000;
    end

    Slope = zeros(size(TrialArray,1),1) * NaN;

    for jj = 3 : size(Slope,1) - 3;
        Slope(jj) = (Concentration(jj+2) - Concentration(jj-2))/
(TrialArray(jj+2,2) - TrialArray(jj-2,2));
        if Slope(jj) == 0;
            Slope(jj) = NaN;
        end
    end

    ChangeInSlope = zeros(size(TrialArray,1),1) * NaN;

    for jj = 1 : size (ChangeInSlope,1) -1;
        ChangeInSlope(jj) = (Slope(jj+1) - Slope(jj))/
(TrialArray(jj+1,2) - TrialArray(jj,2));
        if ChangeInSlope(jj) == 0;
            ChangeInSlope(jj) = NaN;
        end
    end

    MaxConcentrationArray(ii) = max(PressureCorrection);
    MinConcentrationArray(ii) = min(PressureCorrection);
    MaxHumidityArray(ii) = max(TrialArray(:,6));
    MinHumidityArray(ii) = min(TrialArray(:,6));
    MeanTemperatureArray(ii) = mean(TrialArray(:,4));
    MinPressureArray(ii) = min(TrialArray(:,5));
    DiffPressureArray(ii) = (mean(TrialArray(1:20,5)) -
min(TrialArray(:,5)));
    FinalTrialArray = [TrialArray(:,1:3) PressureCorrection
Concentration Slope ChangeInSlope TrialArray(:,4:6)];
end

%% Prepare data for Python Modeling
RegArray = FinalTrialArray;
for ii = 1 : size(TrialArray,2);
    RegArray = RegArray(:, [2,3,9]);
    [numb,Ind] = min(RegArray(:,3));
    TimeShift(ii) = RegArray(Ind,1);
    ConcShift(ii) = RegArray(Ind,2);
    RegArray(1:Ind,:) = [];
```

```
    RegArray = [RegArray(:,1)-RegArray(1,1) RegArray(:,2:end)];
    RegArray = [RegArray(:,1) RegArray(:,2)-RegArray(1,2)
RegArray(:,3:end)];
    Indicies = find(RegArray<0);
    [I_row, I_col] = ind2sub(size(RegArray),Indicies);
    RegArray(I_row,:) = [];
    Indicies2 = find(isnan(RegArray));
    [I_row2, I_col2] = ind2sub(size(RegArray),Indicies2);
    RegArray(I_row2,:) = [];
end

%% OUTPUT- Export flux data into Excel files
outname = 'FilteredRaw.xlsx';
tempname = 'DataTransfer.xlsx';
MainHeader = {'Counter' , 'Time(s)' , 'RConc.ppm)' , 'PConc.(ppm)',
'FConc.(ppm)' , 'ChangeInConc.' , 'ChangeinSlope' , 'Temperature(C)' ,
'Pressure(hPa)' , 'Humidity(%)'};
SummaryHeader = {'Trial' , 'MaxConcentration' , 'MinConcentration' ,
'MaxHumidity' , 'MinHumidity' , 'MeanTemperature' , 'MinPressure' ,
'PressureDif' , 'TimeShift' , 'ConcShift'};
TempHeader = {'X' , 'Y', 'P'};

for ii = 1 : size(TrialArray,2);
    xlswrite(outname,MainHeader,ii,'A1');
    xlswrite(outname,FinalTrialArray,ii,'A2');
end

xlswrite(outname,SummaryHeader,ii+1,'A1')   %Write the header name
horizontally
xlswrite(outname,transpose(1:size(TrialArray,2)),ii+1,'A2');  %Write the
trial number
xlswrite(outname,MaxConcentrationArray,ii+1,'B2');    %Write the Summary
values next to each trial number
xlswrite(outname,MinConcentrationArray,ii+1,'C2');
xlswrite(outname,MaxHumidityArray,ii+1,'D2');
xlswrite(outname,MinHumidityArray,ii+1,'E2');
xlswrite(outname,MeanTemperatureArray,ii+1,'F2');
xlswrite(outname,MinPressureArray,ii+1,'G2');
xlswrite(outname,DiffPressureArray,ii+1,'H2');
xlswrite(outname,TimeShift,ii+1,'I2');
xlswrite(outname,ConcShift, ii+1, 'J2');

for ii = 1 : size(RegArray,2);
    xlswrite(tempname,TempHeader,ii,'A1');
    xlswrite(tempname,RegArray,ii,'A2');
end

system('python NonLinearReg.py')

%% End Program
disp 'End'
rehash
toc
```

B3- Python™ code for modeling of first order response

```
import numpy as np
from scipy.optimize import curve_fit
import pandas as pd
import matplotlib.pyplot as plt
from openpyxl import load_workbook
import xlrd

# define 1st order model
def func(t, C, a, u):
    return C * (1 - np.exp(-a * (t-u) ))

for i in xrange(100):
    try:
        df = pd.read_excel(r'F:\Masters Work\RSCA Project\RSCA
Results\RSCA Matlab Processing\DataTransfer.xlsx',"Sheet%d" %(i+1))
    except xlrd.XLRDError as e1:
        print "ERROR: %s" % str(e1)
        Size = i
        break

ArraySS = np.ndarray((Size,1))
ArrayTC = np.ndarray((Size,1))
ArrayTO = np.ndarray((Size,1))

for i in xrange(Size):
    df = pd.read_excel(r'F:\Masters Work\RSCA Project\RSCA Results\RSCA
Matlab Processing\DataTransfer.xlsx',"Sheet%d" %(i+1))
    x = df['X']
    y = abs(df['Y'])
    print(i+1)

    try:
        popt, pcov = curve_fit(func, x, y)
        y_fit = func(x, popt[0], popt[1], popt[2])
#        print popt, pcov
#        plt.scatter(x, y)
#        plt.plot(x, y_fit)
#        plt.show()
        ArraySS[i] = popt[0]
        ArrayTC[i] = popt[1]
        ArrayTO[i] = popt[2]
    except (RuntimeError,TypeError) as e:
        print "ERROR: %s" % str(e)
        ArraySS[i] = 0
        ArrayTC[i] = 0
        ArrayTO[i] = 0

Array = np.concatenate([ArraySS,ArrayTC,ArrayTO],axis=1)
index = np.arange(1,Size+1)

df2 = pd.DataFrame(data=Array, index=index, columns=('SS','TC','TO'))

book = load_workbook('F:\Masters Work\RSCA Project\RSCA Results\RSCA
Matlab Processing\FilteredRaw.xlsx')
```

```
writer = pd.ExcelWriter('F:\Masters Work\RSCA Project\RSCA Results\RSCA
Matlab Processing\FilteredRaw.xlsx', engine='openpyxl')
writer.book = book
writer.sheets = dict((ws.title, ws) for ws in book.worksheets)

df2.to_excel(writer, "Sheet%d" %(Size+2))

writer.save()
```

B4- SAS code for section 3.1 Sensor Testing

```
PROC IMPORT OUT= WORK.Field26SensorTest
            DATAFILE= "F:\Masters Work\RSCA Project\RSCA
Results\Stats\DATA\Field26SensorTesting.xlsx"
            DBMS=EXCEL REPLACE;
     RANGE="Sensor$";
     GETNAMES=YES;
     MIXED=NO;
     SCANTEXT=YES;
     USEDATE=YES;
     SCANTIME=YES;
RUN;

PROC IMPORT OUT= WORK.BoxesSensorTest
            DATAFILE= "F:\Masters Work\RSCA
Project\BoxExperiment\BoxSensorData.xlsx"
            DBMS=EXCEL REPLACE;
     RANGE="BoxSensorW$";
     GETNAMES=YES;
     MIXED=NO;
     SCANTEXT=YES;
     USEDATE=YES;
     SCANTIME=YES;
RUN;


/*PROC SORT DATA = BoxesSensorTest;*/
/*  BY Compaction ID;*/
/*RUN;*/


PROC GLM DATA = Field26SensorTest;
  CLASS Method;
  MODEL X1-X3 = Method;
  MANOVA H = Method/PRINTE;
  REPEATED Time 3 CONTRAST(1)/SUMMARY;
RUN;

PROC GLM DATA = BoxesSensorTest;
  CLASS Method;
  MODEL X1-X3 = Method;
  MANOVA H = Method/PRINTE;
  REPEATED Time 3 CONTRAST(1)/SUMMARY;
RUN;

PROC PRINT DATA=Field26SensorTest;
```

```
RUN;

PROC PRINT DATA=BoxesSensorTest;
RUN;
```

B-5 SAS code for section 3.3 Field Experiment

```
PROC IMPORT OUT= WORK.FieldData
            DATAFILE= "F:\Masters Work\RSCA Project\RSCA Results\RSCA
Matlab Processing\Filtered\StatsSummary.xlsx"
            DBMS=EXCEL REPLACE;
     RANGE="Complete$";
     GETNAMES=YES;
     MIXED=NO;
     SCANTEXT=YES;
     USEDATE=YES;
     SCANTIME=YES;
RUN;

PROC SORT DATA = FieldData;
  BY Date Site Trial;
RUN;

data FieldData;
set FieldData;
newFlux=log(Flux);
run;

PROC REG DATA = FieldData;
/*  BY Site;*/
  MODEL newFlux = Humidity Temperature Pressure TC Delta1 Delta2 HT HP
HTC HD1 HD2 TP TTC TD1 TD2 PTC PD1 PD2 TCD1 TCD2/p
  SELECTION = stepwise
  SLENTRY = 0.1;
  plot predicted.*newFlux;
  plot r.*p.;
RUN;

PROC REG DATA = FieldData;
/*  BY Site;*/
  MODEL Flux = Humidity Temperature Pressure TC Delta1 Delta2 HT HP HTC
HD1 HD2 TP TTC TD1 TD2 PTC PD1 PD2 TCD1 TCD2/p
  SELECTION = stepwise
  SLENTRY = 0.1;
  plot predicted.*Flux;
  plot r.*p.;
RUN;

PROC PRINT DATA=FieldData;
RUN;

QUIT;
```

B-6 SAS code for section 3.4 Controlled Experiment

```
PROC IMPORT OUT= WORK.BoxPressure
            DATAFILE= "F:\Masters Work\RSCA
Project\BoxExperiment\BoxesStatAnalysis.xlsx"
            DBMS=EXCEL REPLACE;
     RANGE="SASPressure$";
     GETNAMES=YES;
     MIXED=NO;
     SCANTEXT=YES;
     USEDATE=YES;
     SCANTIME=YES;
RUN;

PROC IMPORT OUT= WORK.BoxConcentration
            DATAFILE= "F:\Masters Work\RSCA
Project\BoxExperiment\BoxesStatAnalysis.xlsx"
            DBMS=EXCEL REPLACE;
     RANGE="SASConcentration$";
     GETNAMES=YES;
     MIXED=NO;
     SCANTEXT=YES;
     USEDATE=YES;
     SCANTIME=YES;
RUN;


PROC IMPORT OUT= WORK.BoxConcentrationG
            DATAFILE= "F:\Masters Work\RSCA
Project\BoxExperiment\BoxesStatAnalysis.xlsx"
            DBMS=EXCEL REPLACE;
     RANGE="SASConcentrationG$";
     GETNAMES=YES;
     MIXED=NO;
     SCANTEXT=YES;
     USEDATE=YES;
     SCANTIME=YES;
RUN;

proc mixed data=BoxPressure method=type3;
class Moisture Compaction;
model Pressure = Moisture Compaction Moisture*Compaction;
store PressureOUT;
run;

ods graphics on;
proc plm restore=PressureOUT;
lsmeans Moisture*Compaction / adjust=tukey plot=meanplot cl lines;
ods exclude diffs diffplot;
run; title; run;

proc mixed data=BoxConcentration method=type3;
class Moisture Compaction;
model Concentration = Moisture Compaction Moisture*Compaction;
store ConcentrationOUT;
run;
```

```
proc plm restore=ConcentrationOUT;
lsmeans Moisture*Compaction / adjust=tukey plot=meanplot cl lines;
/* Because the 2-factor interaction is significant, we need to work with
the treatment combination means */
ods exclude diffs diffplot;
run; title; run;

proc mixed data=BoxConcentrationG method=type3;
class Moisture Compaction Glucose;
model Concentration = Moisture Compaction Glucose Moisture*Compaction
Moisture*Glucose Compaction*Glucose Moisture*Compaction*Glucose;
store ConcentrationGlucoseOUT;
run;

proc plm restore=ConcentrationGlucoseOUT;
lsmeans Moisture*Compaction*Glucose / adjust=tukey plot=meanplot cl
lines;
ods exclude diffs diffplot;
run; title; run;

proc plm restore=ConcentrationGlucoseOUT;
lsmeans Moisture*Glucose / adjust=tukey plot=meanplot cl lines;
ods exclude diffs diffplot;
run; title; run;
```

Appendix C: Additional Data

C1- Drop in Pressure (hPa) results for the two factor factorial design with two levels of compaction and four levels of humidity.

	Dry	Low	Medium	High
Compacted	12.01	18.36	18.36	19.37
	13.45	17.78	19.62	19.94
	11.08	16.54	18.44	19.66
	13.67	17.46	18.91	19.25
	14.13	18.33	19.73	16.87
Non Compacted	8.62	8.18	7.48	8.27
	6.82	6.88	7.90	6.82
	8.65	6.30	8.32	11.31
	8.47	7.85	7.17	11.75
	9.73	7.30	7.13	11.88

C2- Change in CO_2 (ppm) results for the two factor factorial design with two levels of compaction and four levels of humidity

	Dry	Low	Medium	High
Compacted	15.1	308.1	674.6	558.6
	21.0	320.4	588.0	465.0
	12.1	304.1	614.5	497.4
	14.6	297.2	532.8	1536.5
	8.3	319.4	568.8	366.9
Non Compacted	53.3	420.8	651.2	2407.7
	27.0	414.1	668.8	1791.5
	22.9	430.5	515.0	1838.6
	40.8	423.6	503.0	1964.8
	48.4	390.3	511.4	1714.5

C-3 Change in CO_2 (ppm) results for the three factor factorial design with two levels of compaction, humidity and presence of glucose.

	Glucose		No Glucose	
	Dry	Wet	Dry	Wet
Compacted	33.0	2065.5	15.1	558.6
	36.1	2307.5	21.0	465.0
	49.9	2621.2	12.1	497.4
	28.1	5511.4	14.6	1536.5
	48.0	1005.3	8.3	366.9
Non Compacted	31.2	3215.9	53.3	2407.7
	31.4	4160.5	27.0	1791.5
	43.6	3969.9	22.9	1838.6
	50.9	4041.0	40.8	1964.8
	31.4	3533.3	48.4	1714.5

C-3 Drop in Pressure (hPa) results for the three factor factorial design with two levels of compaction, humidity and presence of glucose

	Glucose		No Glucose	
	Dry	Wet	Dry	Wet
Compacted	18.40	32.28	12.01	19.37
	18.45	30.65	13.45	19.94
	19.73	32.40	11.08	19.66
	18.08	31.01	13.67	19.25
	19.43	32.07	14.13	16.87
Non Compacted	14.99	18.44	8.62	8.27
	14.05	11.77	6.82	6.82
	14.31	16.06	8.65	11.31
	16.25	14.18	8.47	11.75
	14.05	18.75	9.73	11.88